Graphical Abstract

Operational optimisation of a microgrid using non-stationary hybrid switched model predictive control with virtual storage-based demand management

Grzegorz Maślak,Przemysław Orłowski

Can the cost of microgrid operation be reduced by incorporating virtual storage-based energy management while simultaneously including other vital functionalities in the management system, such as community participation?

Motivation and background

Participation in electricity markets is vital in microgrid management.

Interconnected microgrids offer various benefits, including enhanced energy availability and stability.

Demand management often meets problems with public acceptance and cost allocation.

Virtual storage-based demand management may enhance economic performance and public acceptance.

Methodology

Analysis of control performance in changing modes of operation with consideration of neighbourly energy exchange.

In-depth analysis of system sensitivity to changes in the cost function, prediction accuracy and horizon length.

Comparison of system performance with different types of proposed virtual storage.

Results

A new non-stationary hybrid model of microgrid paired with model predictive control law is proposed.

With the use of the proposed bidirectional virtual storage, the cost of microgrid operation decreases by an average of 16%.

The sensitivity of the system to changes in parameters is low enough to allow adjustment.

Conclusion: The research presented in this study led to the development of a non-stationary microgrid hybrid model. An associated microgrid operation optimisation method based on receding horizon control featuring a new method of demand management is also featured.

Reference: Operational optimisation of a microgrid using non-stationary hybrid switched model predictive control with virtual storage-based demand management, Maślak G., Orłowski P., Renewable and Sustainable Energy Reviews 2024

Highlights

Operational optimisation of a microgrid using non-stationary hybrid switched model predictive control with virtual storage-based demand management

Grzegorz Maślak,Przemysław Orłowski

- The introduction of the virtual energy storage reduces operating costs by up to 16%

- The lowest cost is obtained with bidirectional virtual energy storage

- Demand management operating on two time-scales allows a reduction in generator usage

- Virtual storage allows for fuller use of renewable energy and increased profits

Operational optimisation of a microgrid using non-stationary hybrid switched model predictive control with virtual storage-based demand management

Grzegorz Maślak[a,b,*],   Przemysław Orłowski[b,*]

[a] *West Pomeranian University of Technology in Szczecin, Doctoral School, Piastów 19, Szczecin, 70-310, Poland*

[b] *West Pomeranian University of Technology in Szczecin, Department of Automatic Control and Robotics,Faculty of Electrical Engineering, Sikorskiego 37, Szczecin, 70-313, Poland*

ARTICLE INFO

ABSTRACT

Demand-shaping mechanisms are a key component of modern energy management systems, although not unproblematic. The degree of social acceptance of interference with demand or generation and the ease of integration of various types of non-critical loads depends on the method of their implementation. In addition, the critical load pool typically includes devices with different response times. The energy management systems currently in use often cannot meet user expectations. Especially when considering other vital aspects, such as energy market spread, storage wear, or connection to the utility grid and neighbouring microgrids. The authors adopted an approach of unifying demand side management and response in the form of virtual energy storage. Said store allows for the accommodation of loads operating under differing scheduling horizons. Such a new concept allows management not only in terms of quantity but also in terms of time. The storage is the focal point of a comprehensive energy management system based on switched model predictive control. The receding horizon algorithm relies on a non-stationary hybrid microgrid model. The study compares the operating costs of microgrids with virtual storage, allowing only demand postponement, preponement or bidirectional operation. The energy management system is also examined for sensitivity to changes in the weight matrices of the cost function, horizon length and forecast inaccuracy. Introducing virtual energy storage reduces microgrid operating costs by up to 16%. The decrease in control performance is proportional to the prediction accuracy, and the sensitivity allows for customization.
Word count: 10153

*Corresponding author.

✉ E-mail adress: grzegorz.maslak@zut.edu.pl (G. Maślak); orzel@zut.edu.pl (P. Orłowski)

🌐 (P. Orłowski)

ORCID(s): 0000-0003-4631-9423 (G. Maślak); 0000-0001-6407-9668 (P. Orłowski)

Nomenclature

Abbreviations

DM demand management

DSM demand side management

DSR demand side response

MPC model predictive control

PES physical energy storage

UG utility grid

VES virtual energy storage

Symbols and Units

A system matrix of the state space model

B input matrix of the state space model

C output matrix of the state space model

C_{gen} auxiliary generator operation cost (€)

C_{net} cost associated with transactions on the energy market (€)

D feed-through matrix of the state space model

E_{bat} amount of energy stored in the physical storage (kWh)

E_{bio} energy associated with physical storage charging or discharging (kWh)

E_d energy demand (kWh)

E_{ib} difference between expected and actual energy balance in the microgrid (kWh)

E_{gen} energy provided by the auxiliary generator (kWh)

E_{net} energy exchanged with external grid (kWh)

E_{net}^{req} energy exchange requested by the community (kWh)

E_{ov} energy lost due to physical storage overflow (kWh)

E_{rdf} energy managed by fast demand management (kWh)

E_{rds} energy managed by slow demand management (kWh)

E_{rds}^{τ} energy scheduled to be managed by slow DM in τ time steps (kWh)

E_{res} energy from renewable sources (kWh)

E_{vbat} amount of energy stored in the virtual storage (kWh)

F_b energy acquisition price (€)

F_{gen} auxiliary generation cost (€)

F_s energy selling price (€)

J optimisation-associated cost

J_e economic cost component

J_q quality cost component

J_T terminal cost component

J_u input-associated cost component

J_x state-associated cost component

J_y output-associated cost component

J_Δ state change rate cost

N prediction horizon used in the receding horizon algorithm

PF power factor

Q_T terminal state weight matrix

Q_x main state weight matrix

Q_Δ state rate of change weight matrix

R input weight matrix

S output weight matrix

S_{net} apparent power exchanged with external grid (kVA)

s_e scaling coefficient associated with economic aspects

s_q scaling coefficient associated with quality aspects

s_u scaling coefficient associated with inputs

s_x scaling coefficient associated with state

s_y scaling coefficient associated with outputs

t_{clc} average control calculation time

u input vector

x state vector

x_r reference value of state vector

y output vector

z prediction error

δ_{cs} microgrid connection status with external grid

Θ state associated disturbances matrix

ν_c physical storage charging efficiency

ν_d physical storage discharging efficiency

Ω input associated disturbances matrix

ω disturbances vector

1. Introduction

Electricity will most likely remain the primary energy source in the foreseeable future. Despite that, recent climate and energy policy tends towards reducing greenhouse gas emissions and achieving energy systems without a significant carbon footprint. The aim is to retain a high degree of cost-effectiveness. Prime examples are initiatives such as net zero and carbon targets. A key solution to meeting those goals is the introduction of resilient grids. Said grids should incorporate complex storage capabilities with the widespread usage of various renewable energy sources. Transition to such means is a crucial factor in sustainable global development [1] and is already taking place. Yet such an adoption is not trivial due to challenges arising from user demands and fluctuating wind or solar power profiles. Those profiles are far different from steam

turbines, as pinpointed in [2, 3]. Further challenges emerge due to the often outdated classic distribution grid void of capacity needed to support rising consumer needs and the increasing number of small power sources. The desire to be independent of the grid while retaining local reliability, low cost and power quality, even in areas lacking the infrastructure, poses further problems [4]. The low-level structural solution to those new challenges is to split the electrical network into smaller segments based on distributed resources. Every smaller segment should act as a single controllable entity, the so-called microgrid. It manages the local loads and generation, is equipped with storage capabilities, and is often interconnected locally [5, 2]. Microgrids emerge as a flexible solution to the problems and challenges mentioned, offering a local solution having several functional edges over the conventional centralised system [6]. However, such a solution requires proper control.

The general concept of virtual energy storage (VES) is already well established. However, its very definition and role in the control system differ from work to work. Appropriate energy management facilitates the reduction of surplus generation from non-renewable sources and its substitution with renewable energy. Consequently, using advanced control systems in microgrids enables greater efficiency by balancing demand with available supply [7]. Thus, more renewable energy is used during peak demand with proper system management. Thereby avoiding meeting at least some of the customer needs with non-renewable energy sources. Further gains can be made by incorporating adequate storage capabilities, market dynamics awareness, and demand management (DM). Virtual energy storage can be deemed an important element of microgrid control associated with DM. This storage type is often linked with an energy-consuming process involving some indirect storage medium. Water desalination installations powered with renewable energy, as proposed by authors of [8, 9], can be considered a typical example. Other examples include the solution introduced in [10], which also uses the principle of substitute energy storage medium, namely a belt conveyor system with a coal silo. A slightly different approach is presented in [11], where a joint water and electricity supply system is considered. Further examples include the usage of the electric vehicle fleets [12, 13] or thermodynamic processes [14, 15, 16]. All those solutions concern virtual energy stores tied to a specific medium and system layout. Certain works define VES in alternative ways. Stores included in [17] and [18] are derived as an energy storage model based on circuit theory and the droop control algorithm. Despite analogous assumptions, this type of approach is unsuitable for high-level management. As demonstrated in [19], the VES can also be generalised to a form that intends to shape user behaviour through energy prices. The suitability of applying specific optimisation or control algorithms depends on the VES integration method. The same principle applies to DM with different time scales. Authors recognise the lack of solutions oriented towards generalizing the VES to any medium and, at the same, making it suitable for consumers with different response times.

The set of features to be implemented in energy management systems based on optimisation is not strictly defined. However, in the case of economic optimisation, some form of DM can be considered core functionality. Demand management usually takes place under the control of some algorithm or as part of a broader control system. Different optimisation methods are used depending on how the problem is formulated and how the microgrid elements and its operating environment are described. As demonstrated in [20, 21], optimal DM can be formulated as linear or nonlinear programs. Such programs are solvable using diverse methods, including mixed integer programming, heuristic, meta-heuristic algorithms, or game theory. For end-to-end solutions including DM, model predictive control (MPC) is a frequent choice [22, 23]. Generally, a common approach is the diversely understood scheduling of energy utilisation. Many works group energy consumers and recognise the need to influence them with different intensities and schedules. Examples include [24, 25], where the need for control across more than one time scale is distinguished. In addition, processes similar to a VES in the form of thermal energy storage or electric cars are introduced. The energy market is integrated with a spread, but direct DM is not implemented. A bipartite scheduling concept applies to the control law with high energy market integration but omits advanced DM as presented in [26]. Similarly, authors of [27] identify a range of consumers subject to DM and response mechanisms. However, dynamic constraints are not applied, and physical energy storage (PES) wear is not considered. Both solutions operate only in on-grid mode and consider the market spread. A proposal for a solution dedicated to the off-grid operation equipped with extensive battery consumption criteria but with only generation reduction

Table 1
A summary of selected features included in optimisation-based energy management systems proposed in other works.

Feature	[24]	[25]	[26]	[27]	[28]	[30]	[32]	[33]	[35]	[36]	[37]	[38]	[39]	[40]	[41]
virtual energy storage	+	+	-	-	-	-	-	-	-	-	-	-	-	-	-
multi time-scale demand management	-	-	+	+	-	-	-	-	-	-	-	-	-	+	-
energy market spread	+	+	+	+	-	-	+	-	-	-	-	+	-	+	-
flexible demand management constraints	-	-	-	-	-	-	-	-	-	-	-	+	+	-	+
physical storage wear	-	+	-	-	+	-	+	+	-	+	-	+	+	-	+
model predictive control	+	+	+	-	+	-	+	+	-	+	+	+	+	+	+

capabilities is found in [28]. A two-level economic approach to energy management suitable for on-grid microgrids participating in the electricity market but without the energy market spread is introduced in [29]. Distributed DM problem using game theory supported by block-chain is proposed in [30], although PES wear and market spread are not considered. The importance of considering energy exchange between neighbouring microgrids is consulted in [31]. The authors integrate singular dynamic energy pricing and PES wear minimisation. Both are paired with demand time-shifting, allowing demand reduction, and with varying constraints designed so that the reduction does not exceed the current demand. The VES concept is not used as in [32]. Here, the authors include the ability to switch between islanded and on-grid operation modes. Aside from PES wear consideration, also recognised in [33], multiple instantaneously operating non-critical loads are presented. An approach based on switched MPC is proposed in [34]. There is no consideration of the electricity market spread between the bid and ask prices, similar to the decision tree solution developed in [35]. Given many microgrids operate under intermittent or no public grid access, considerable work focuses exclusively on off-grid mode where storage life is important [36]. One example is [37], where aside from off-grid operation, the focus is on prediction inaccuracy. The picture that emerges is a lack of solutions simultaneously considering the energy market spread, advanced demand shifting, community mode, and reduction of PES wear in the optimisation problem. Moreover, most of the works focus on a specific mode of operation. On the contrary, comprehensive solutions are presented in [38] and [39]. Still, they do not introduce multiple scheduling horizons, or there is only demand reduction and no integration of separate energy bid and ask prices. A further example is the work [40]. An advanced solution covering twin-shift scheduling based on two optimisers is shown. The authors mention the VES and introduce market spread but do not consider flexible demand reduction constraints or PES wear. Table 1 summarises selected functionalities implemented in energy management systems featured in other works. Subsequently, the unification of DM and its inclusion with complex MPC law allows for a universal and scalable solution that corresponds well with receding horizon algorithms. Moreover, participation in the balancing energy market increases the overall share of renewable energy in the energy mix.

The results presented in this work are intended to prove that it is possible to reduce the cost of microgrid operation by incorporating the proposed VES-based DM while simultaneously including various other functionalities in the energy management system. These features include key aspects such as participation in the energy market, energy exchange with neighbouring microgrids, different response times of loads subject to demand shaping and minimising PES wear. In addition, the solution is to use control law switching to adjust the control to the mode of operation. Particular emphasis is placed on developing a comprehensive way to manage energy demand based on a VES. The suggested solution is also to combine the DM in terms of time and quantity. The authors intend to answer some of the problems pinpointed in [42, 22, 43] regarding the construction of complex microgrid models. This is accomplished using hybrid systems modelling and by the introduction of a non-stationary element as well as the adoption of MPC control law. Moreover, the proposed system should increase the share of consumed renewable energy by optimal usage of both VES and PES. The resulting receding horizon problem includes varying constraints. The maximal amount of energy subject to fast DM depends on actual and predicted demand. Consequently, the contribution of this study can be characterised as:

- the concept of switched microgrid control incorporating community mode and all features listed in Table 1 in the underlying optimisation problem.

- non-stationary hybrid microgrid model featuring DM with two distinctive time-scales based on the proposed bidirectional VES

- in-depth analysis of the influence of different VES configurations on microgrid operation

- investigation of effects of energy demand and generation predictions inaccuracies and control horizon length on energy management performance

The remainder of this work is organised as follows. The second section describes the non-stationary microgrid hybrid model in state space form, including the VES and energy market. The third section features the control concept, control system configuration, and receding horizon optimisation problem. The fourth section illustrates the methodology employed to scrutinise the performance of the proposed solution. Afterwards, the control system is trialled in changing connection mode. Firstly, the solution sensitivity regarding cost function weighting matrices and the influence of prediction horizon length is investigated. Secondly, the impact of forecast accuracy and the importance of the allowed direction of VES charging are examined. Lastly, conclusions are made, and the scope of future research is elucidated.

2. Economically oriented microgrid hybrid model

The term microgrid is usually used to describe a customer-owned facility. Such a facility combines generation, consumption, and power exchange management between the microgrid and the utility grid (UG). It can also switch between islanded and on-grid modes [2]. As mentioned earlier, the definition can refer to various types of clients depending on the scale. Those can be a single low-voltage domestic customer, groups of customers supplied by medium-voltage lines and even large groups of consumers connected to a high-voltage grid. Every microgrid requires appropriate control systems to ensure, among other things, stabilisation of grid voltage and frequency, reactive power compensation and spinning reserve. Any control systems, therefore, have to face many problems, including those arising from the diversity of the control objective and time scale. According to [22], hierarchical control is the answer to this challenge.

Said systems consist of three distinguishable levels [2]. Primary control stabilises the frequency and voltage in response to rapid load changes, thus operating on the smallest timescale. Secondary control focuses on nullifying grid parameter deviations in steady-state. It also concentrates on synchronising with the UG after transitioning to on-grid operation. Lastly, tertiary control is responsible for power flow control between microgrid elements or between microgrid clusters and upstream UG. This research focuses on the tertiary control level. The proposed method is intended to allocate energy optimally for several hours ahead. This requires the assumption that signals such as energy prices are constant over a sampling time of one hour. For the study, it is assumed that primary and secondary-level control algorithms operating with significantly shorter sampling times ensure voltage and frequency stabilisation, among others. Constraints of active power must be chosen so that the allowable values of apparent power and line current limits are not exceeded. Admissible power factor values are also important. The selection of these constraints depends on the physical conditions of the microgrid in question. For control purposes, knowing the microgrid model limits and parameters is essential.

The proposed microgrid model covers three operation modes that differ from each other in connection status with the UG and the occurrence of energy exchange within the neighbourhood. On-grid mode is considered the default operation routine. In this mode, the microgrid can freely exchange energy with the UG. Such a UG is understood as a public power network under the control of an independent, third-party operator. It can perform bidirectional transactions with the microgrid under consideration, and all trades are held under the energy market conditions. Within the framework of this work, the energy market is understood to operate hourly. A new price is set every hour based on the relation between energy supply and demand. Some examples of markets operating on this principle can be found in [44]. Additionally, the

authors assume that the microgrid analysed in this work can exchange energy with at least one neighbouring microgrid. A dedicated high-level control system manages energy transfers between community members. Both off-grid and community modes are considered emergency modes. Hence, the times of switching to said modes and returning to on-grid operation are unknown. During emergencies, the high-level control system can request the microgrid to send or receive a specific amount of energy. The price of energy exchanged this way is not taken into account in the optimisation problem. Financial matters concerning emergencies are settled by the operator following the regulations applicable in a given country. When, despite the emergency, energy exchange with neighbours does not occur, or the microgrid is physically disconnected from the grid, authors deem it an off-grid operation. In that case, the microgrid should sustain itself through renewable energy sources or auxiliary power generators. Authors find the introduction of community mode necessary, given the growing importance of energy grids consisting, among others, of many interconnected microgrids. As a result, the operation mode depends on common coupling status δ_{cs} and the amount of energy required to be exchanged with external grids, namely E_{net}. Any voluntary energy exchange is treated as on-grid mode. Figure 1 shows the conditions for switching between the different modes of operation.
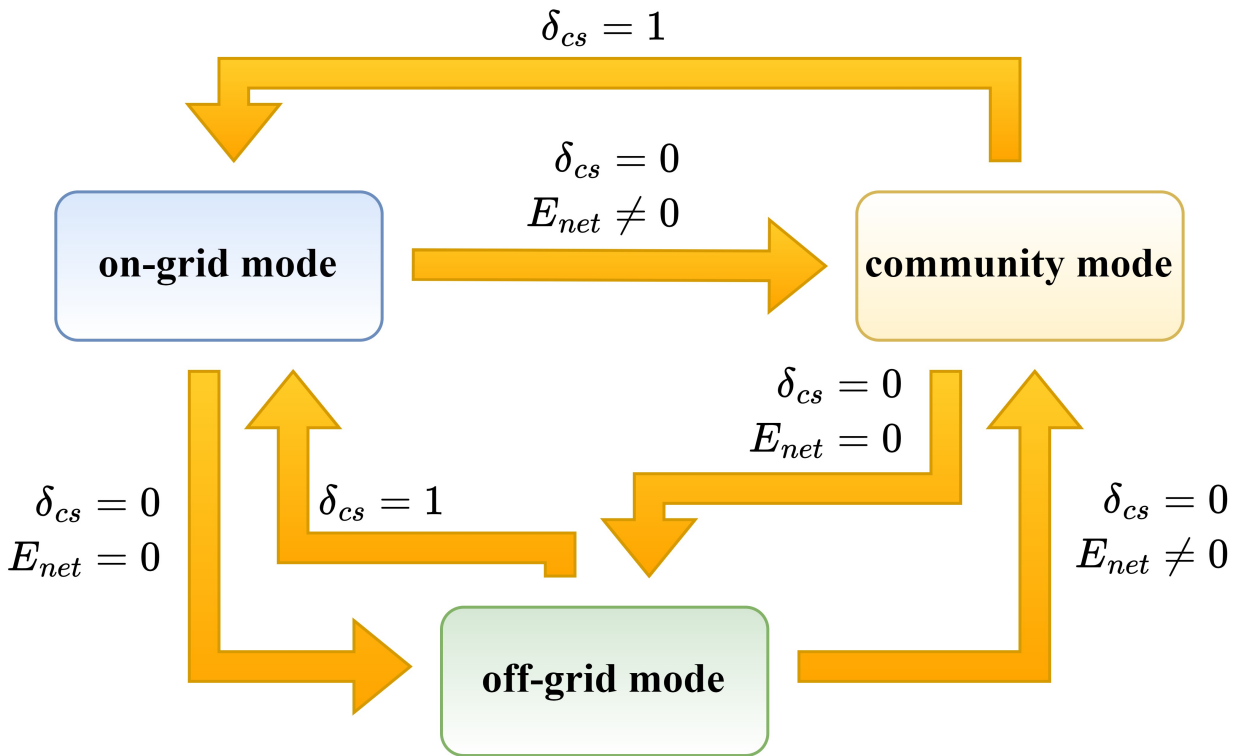
Figure 1: Conditions for switching between modes of microgrid operation.

The proposed model is intended to cover the broadest range of applications possible through its generalised form. The microgrid is coupled with the utility and community grid through the point of common coupling. It possesses the ability to detect power loss and receive information concerning the needs of the community. Renewables are the primary unstable energy source in the target microgrid. Microgrids are often equipped with PES means to mitigate such instability and enhance microgrid reliability and energy availability. Examples are batteries, hydrogen systems and flywheels. In this study, two types of energy storage are considered, the first being the PES and the second being VES. The latter accumulates time-shifted energy demand resulting from the implementation of active DM. Besides, auxiliary power generators are used mainly in times of energy shortages. The authors assume a generalised, summed energy demand with the possibility of load management in a timely and qualitative manner. Finally, a microgrid management

Figure 2: Schematic diagram of the considered microgrid configuration.

system is, in our scope, a control algorithm that considers economic and qualitative aspects. Its main task is to assure appropriat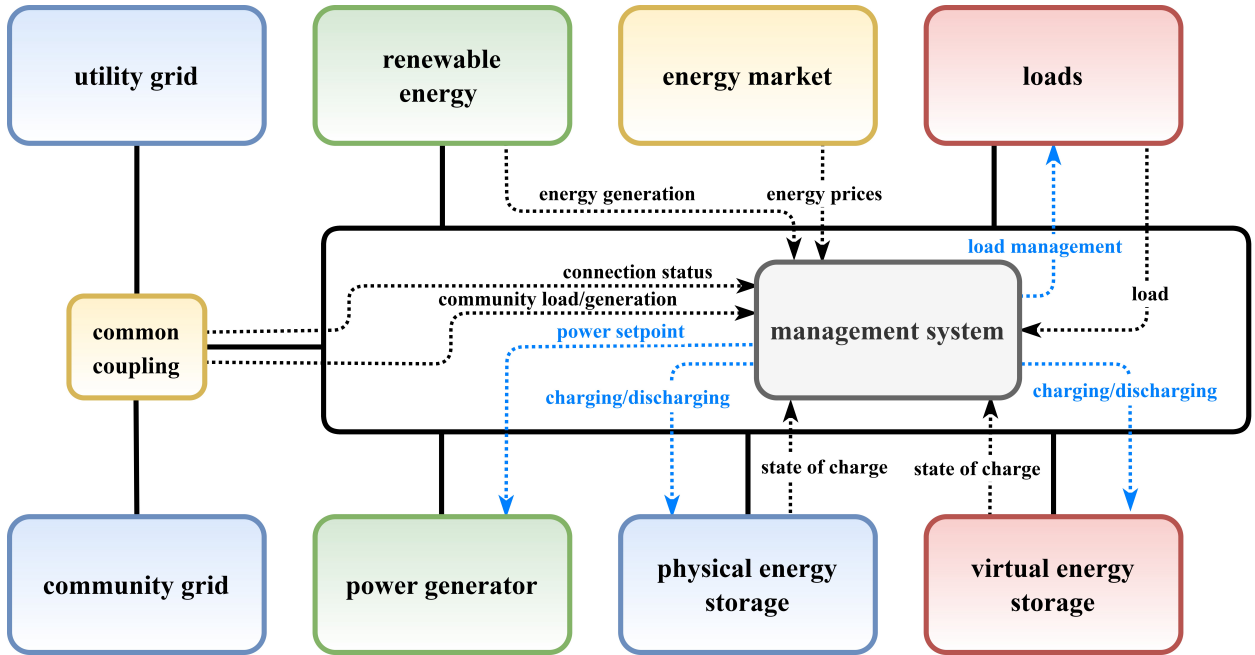e operation stability and maximum utilisation of renewable sources while also taking advantage of market fluctuations. Furthermore, in off-grid mode, the management system should maximise the time the microgrid can autonomously operate. At the same time, in community mode, mandatory exchange with the community grid must be adequately taken into account. Figure 2 shows the diagram of the generalised microgrid and control configuration just described with the addition of basic information flow indication.

2.1. Model equations in on-grid mode

Due to the intended use of hybrid discrete state space representation, the energy flow in the microgrid is described using difference equations and based on energy balance. Physical energy storage can be considered one of the key elements of the microgrid. This stems from the fact that the PES acts as an energy buffer. The amount of stored energy $E_{bat}(k+1)$ depends on the previous amount of energy stored in the PES $E_{bat}(k)$ reduced or increased by the amount of energy discharged or charged $E_{bio}(k)$ with efficiency η_d or η_c, diminished by a constant PES self-discharge E_{sd}. Consequently, in the case of positive $E_{bio}(k)$, energy is stored, while its negative values indicate PES discharge. Equation 1 describes the relationship.

$$E_{bat}(k+1) = E_{bat}(k) + \eta(k)E_{bio}(k) - E_{sd} \tag{1}$$

Moreover, the charging and discharging efficiency $\eta(k)$ depends on the sign of $E_{bio}(k)$. When $E_{bio}(k)$ is positive, the PES is charged with efficiency η_c. If not, the amount of stored energy is reduced with efficiency η_d, as specified in Equation 2.

$$\eta(k) = \begin{cases} \eta_c & \text{for } E_{bio}(k) > 0 \\ \frac{1}{\eta_d} & \text{otherwise} \end{cases} \tag{2}$$

Following [45], demand side management (DSM) and demand side response (DSR) functionalities greatly benefit the microgrid during peak demand hours and contingencies. Both mechanisms also increase end-user affordability and reliability by reducing or postponing load. Such functionalities are often paired with various types of VES. In the scope of this study, the authors define the VES as a storage of energy
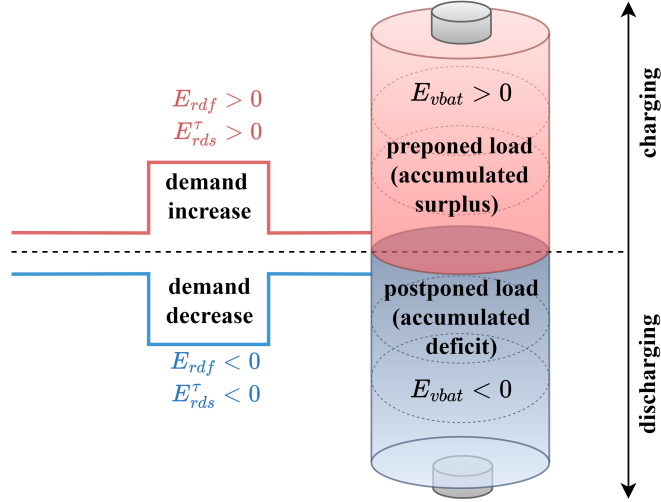
Figure 3: Energy flow in the virtual energy storage.

demand shifted in terms of time using DSR and DSM. This functionality aims to shape the demand appropriately through its reduction or increase. At the same time, it is deemed essential to retain the knowledge of the amount of load denied to or enforced upon the recipient. This allows the load to be shifted over time, assuming that all energy subjected to both forms of shaping is stored in a VES. First of all, two types of quantitative DM mechanisms are considered in the mathematical model. The first is the fast energy management $E_{rdf}(k)$ operated by the control system. It works with a delay of one time-step, while the second type is the slow management $E_{rds}^{\tau}(k)$, which has a significant time delay τ. The intention is to achieve both fast response and planning capability. Such a representation allows DSR and DSM to be generalised to a common form. Figure 3 shows energy transactions with the VES. As shown in Figure 3, positive values of $E_{vbat}(k)$ reflect preponed load. Charging the VES can be associated with using additional energy in advance without specifying the medium. For instance, preheating the water when conditions are favourable and is achieved by momentarily increasing the demand using $E_{rdf}(k)$ and $E_{rds}^{\tau}(k)$. On the contrary, negative values of $E_{vbat}(k)$ are associated with postponed energy demand, which must be met later. Discharging the VES involves reducing the energy demand by employing $E_{rdf}(k)$ and $E_{rds}^{\tau}(k)$. Notably, the authors call the VES bidirectional. The reason is that in the case of accumulation of surplus energy, the only method to reduce the state of charge of the VES is to start creating a deficit with the help of DM. Similarly, in the case of a deficit accumulation, the current demand must be increased to start paying off the debt. The actual degree and direction of resulting demand time-shifting are then expressed through the VES state of charge E_{vbat}, as defined in Equation 3.

$$E_{vbat}(k+1) = E_{vbat}(k) + E_{rds}^{\tau}(k) + E_{rdf}(k) \tag{3}$$

As already mentioned, $E_{rds}^{\tau}(k)$ describes the amount of energy scheduled to be time-shifted τ time steps prior. Such an understanding of the demand response procedure entails the need to introduce scheduling functionalities in the microgrid model. Control signal $E_{rds}(k)$ implies the amount of energy requested to be time-shifted at the time $k + \tau$ and is initially scheduled using $E_{rds}^{1}(k)$. Then, the request is propagated until it reaches $E_{rds}^{\tau}(k)$. Such a scheduled amount of energy finally influences the energy balance, as in Equations 4 through 6. An example of a commercial operator operating under DSR principles, which inspired this part of the model, can be found in [46].

$$E_{rds}^{1}(k+1) = E_{rds}(k) \tag{4}$$

$$E_{rds}^{2}(k+1) = E_{rds}^{1}(k) \tag{5}$$

$$\vdots$$

$$E_{rds}^{\tau}(k+1) = E_{rds}^{\tau-1}(k) \tag{6}$$

The focal point of energy flow in on-grid mode is the common coupling point through which the microgrid exchanges energy with the UG. The UG, in this case, serves as a convenient balancing medium. As a result, any intentional or non-intentional imbalance in the microgrid is suppressed using energy bought from or sold to the UG. Planed energy stock exchange transactions under the balancing market conditions are necessary to optimise microgrid operation economically. However, some unplanned energy exchange with the UG must occur in real-life conditions to mitigate disturbances. Those can include finite model accuracy, imprecise demand and renewable energy generation forecasts. Microgrid management systems often utilise forecasts concerning energy demand and generation. The bearing of some forecast error is typical for this type of data. Hence, the authors find it necessary to take that into account. To demonstrate, Equations 7 and 8 describe renewable energy influx and energy demand, respectively. Variables $\hat{E}_{res}(k)$ and $\hat{E}_d(k)$ exemplify forecasts made for a given time step while $z_{res}(k)$ and $z_d(k)$ correspond to individual forecasting errors. Thus, the sum of the forecast value for a given variable and the error with which this forecast is entailed describes the actual value of the variable. Besides, such a notation allows additional sources of error to be considered. For instance, the averaging error results from assuming that energy balance components are constant over the sampling period. Nevertheless, said approach will be applied to other variables included in the energy balance.

$$E_{res}(k) = \hat{E}_{res}(k) + z_{res}(k) \tag{7}$$

$$E_d(k) = \hat{E}_d(k) + z_d(k) \tag{8}$$

Consequently, actual energy exchanged with UG $E_{net}(k)$ can be defined as a balance between energy generation, energy demand reduced or increased by DM and PES charge or discharge. Firstly, two primary energy sources are considered - renewable energy production $E_{res}(k)$ and generator output $E_{gen}(k)$. Secondly, the energy demand $E_d(k)$ can be diminished or increased by postponed or preponed loads $E_{rds}^{\tau}(k)$ and $E_{rdf}(k)$. Subsequently, additional energy can be introduced or drained through transactions with the PES, described using $E_{bio}(k)$. Lastly, the variable $E_{ov}(k)$ corresponds to safety systems and simultaneously allows the solution to remain feasible. If renewable energy is lost due to PES overflow, $E_{ov}(k)$ takes on negative values. Conversely, positive values indicate a deficit of energy in the balance. Thus, the defined balance in the microgrid is described by Equation 9.

$$\begin{aligned} E_{net}(k) = E_{res}(k) + E_{gen}(k) - E_d(k) + E_{rds}^{\tau}(k) \\ + E_{rdf}(k) - E_{bio}(k) + E_{ov}(k) \end{aligned} \tag{9}$$

What follows, the principle described in Equations 7 and 8 can be applied to the energy balance presented in Equation 9. Thus, the difference between the forecasted $\hat{E}_{net}(k)$ and the actual value of the balance $E_{net}(k)$ will be the disturbance $z(k)$ as depicted in 10.

$$E_{net}(k) = \hat{E}_{net}(k) + z(k) \tag{10}$$

The disturbance $z(k)$ is the sum of errors for the individual variables present in Equation 9. This relation is described by Equation 11.

$$z(k) = z_{res}(k) + z_{gen}(k) - z_d(k) + z_{rds}^{\tau}(k) + z_{rdf}(k) - z_{bio}(k) + z_{ov}(k) \tag{11}$$

As a rule, in on-grid mode, energy described as $z(k)$ must be balanced through the UG. This, in turn, leads to the introduction of the imbalance $E_{ib}(k)$, bringing together the disturbances which enforce the unintended energy exchange with the UG. As a consequence, Equations 10 and 12 describe the relation between energy exchange and imbalance.

$$E_{ib}(k) = z(k) \tag{12}$$

Lastly, it should also be noted that Equation 9 includes negative $E_{bio}(k)$. Considering the physical sense of $E_{bio}(k)$, the amount of energy discharged from PES must increase the value of $E_{net}(k)$ but decrease the PES level described in Equation 1, hence the negation.

Due to the planned economic optimisation, some cost measures are required. Two primary operation cost sources are related to energy exchange and conventional power generator operation costs. Transactions with the UG can generate costs associated with energy purchases and create income through energy sales. Therefore, associated cost or income measure $C_{net}(k)$ may take positive values to indicate cost or negative to imply income. Moreover, as a rule of the balancing market, energy prices change over time. For this reason, the energy price $F_{net}(k)$ included in Equation 13 is defined as a time-dependent variable.

$$C_{net}(k) = -F_{net}(k)E_{net}(k) \tag{13}$$

What is more, to account for the energy market spread, $F_{net}(k)$ alternates between the expected purchase price $\hat{F}_b(k)$ and selling price $\hat{F}_s(k)$ in line with the direction of energy transactions. Thus, the model considers the spread of the market, as highlighted in the contribution. Energy is sold to the UG when $E_{net}(k)$ is positive and bought in all other cases, as defined in Equation 14.

$$F_{net}(k) = \begin{cases} \hat{F}_s(k) & \text{for } E_{net}(k) > 0 \\ \hat{F}_b(k) & \text{otherwise} \end{cases} \tag{14}$$

Likewise, generator operation cost $C_{gen}(k)$ is given by Equation 15. The product of constant combined operation cost coefficient F_{gen} and generator output $E_{gen}(k)$ yields said cost.

$$C_{gen}(k) = F_{gen}E_{gen}(k) \tag{15}$$

2.2. Model equations in off-grid and community mode

The dynamics of the phenomena that make up the description of the microgrid in off-grid mode bear a strong resemblance to that in on-grid mode. However, the inability to exchange energy with the grid is a significant difference. As a result, the disturbance mitigation through the UG becomes impracticable. Thus, energy balance fluctuations are compensated by using PES instead of performing transactions with the UG. For the most part, this statement is true for both off-grid and community modes. Regarding the mathematical description, the total energy exchanged in off-grid mode must equal zero. This means isolation from potential external energy consumers and suppliers such as neighbours or the UG. Conversely, in the community mode, the microgrid must provide or receive a set amount of energy, which implies non-zero total energy exchange. This constitutes the fundamental difference between the two modes. However, mandatory neighbourly exchange E_{net}^{req} can be treated as a priority load or demand not subject to management. As a result, the description of these modes can be generalised. Nonetheless, bearing in mind the versatility of the model, the authors want to emphasise the significance of the community mode. The amount of energy stored in the battery in off-grid and community mode depends on the previous amount of stored energy $E_{bat}(k)$ reduced or increased by compensated disturbances $z(k)$. In this case, the PES must be used for such balancing purposes. Consequently, efficiency $\eta(k)$ prescribes the PES efficiency. Furthermore, a constant E_{sd} determines the extent of self-discharge, as shown in Equation 16.

$$E_{bat}(k+1) = E_{bat}(k) + \eta(k)(E_{bio}(k) + z(k)) - E_{sd} \tag{16}$$

Switching between charging and discharging efficiencies should include disturbances $z(k)$. For this reason, the modified definition of $\eta(k)$ is described using Equation 17.

$$\eta(k) = \begin{cases} \eta_c & \text{for } E_{bio}(k) + z(k) > 0 \\ \frac{1}{\eta_d} & \text{otherwise} \end{cases} \tag{17}$$

The microgrid must meet the mandatory energy exchange imposed by the community. For that reason, the imbalance $E_{ib}(k)$ in off-grid and community mode equals not only the disturbances $z(k)$ but also contains the difference between the energy bound to be exchanged with the community $\hat{E}_{net}$ and the actual amount of energy requested $E_{net}^{req}(k)$. Thus, the imbalance in off-grid mode is given by Equation 18

$$\begin{aligned} E_{ib}(k) = &\hat{E}_{res}(k) + \hat{E}_{gen}(k) - \hat{E}_d(k) + E_{rds}^{\tau}(k) \\ &+ \hat{E}_{rdf}(k) - \hat{E}_{bio}(k) + \hat{E}_{ov}(k) - E_{net}^{req}(k) + z(k) \end{aligned} \tag{18}$$

The dependencies that characterise the imbalance can be further simplified by utilising Equation 9, which still holds in off-grid mode. A simplified form of this relationship is expressed using Equation 19

$$E_{ib}(k) = \hat{E}_{net}(k) - E_{net}^{req}(k) + z(k) \tag{19}$$

In the community mode, $E_{net}(k)$ indicates the energy exchanged with the community instead of the UG. Furthermore, $\hat{E}_{net}(k)$ has to strictly match the requested amount of energy $E_{net}^{req}(k)$. This shall be achieved through appropriate control. Apart from this, during off-grid operation, $E_{net}^{req}(k)$ must be constantly set to zero. Consequently, the associated cost or income measure $C_{net}(k)$ in both operation modes equals zero, given that no external energy exchange occurs. Yet, the generator operation cost is described as analogous to the on-grid mode using Equation 15. Similarly, Equation 3 is used to describe the VES in on-grid mode along with Equations 4 through 6, which still hold. The authors decided not to repeat those redundant relationships. Significantly, all three microgrid operation modes are described so that resulting state space representations are compatible with each other when the switchover between operation modes occurs. Moreover, the general interpretation of all the variables remains the same.

2.3. Microgrid state space representation

The expressions described in Subsections 2.1 and 2.2 are rearranged into a more concise state space description. This description type is chosen mainly because of the prospect of using model-predictive control. Due to the energy market and PES dynamics, the proposed state space model is hybrid and non-stationary. The hybridity is determined by the PES charging and discharging and by the sale and purchase of energy. Apart from this, the dynamic price imposed by the balancing energy market determines the non-stationarity. The expression 20 describes the resulting non-stationary hybrid state space model.

$$
\begin{aligned}
x(k+1) &= \\
&\begin{cases}
A_{off}x(k) + B_{off}^c(k)u(k) + \Omega_{off}^c\omega(k) & \text{for } \sim\delta_{cs}(k) \wedge E_{bio}(k) + z(k) \geq 0 \\
A_{off}x(k) + B_{off}^d(k)u(k) + \Omega_{off}^d\omega(k) & \text{for } \sim\delta_{cs}(k) \wedge E_{bio}(k) + z(k) < 0 \\
A_{on}x(k) + B_{on}^c u(k) + \Omega_{on}\omega(k) & \text{for } \delta_{cs}(k) \wedge E_{bio}(k) \geq 0 \\
A_{on}x(k) + B_{on}^d u(k) + \Omega_{on}\omega(k) & \text{for } \delta_{cs}(k) \wedge E_{bio}(k) < 0
\end{cases} \\
y(k) &= \begin{cases}
C_{off}(k)x(k) + D_{off}(k)u(k) + \Theta_{off}(k)\omega(k) & \text{for } \sim\delta_{cs}(k) \\
C_{on}^s(k)x(k) + D_{on}^s(k)u(k) + \Theta_{on}^s(k)\omega(k) & \text{for } \delta_{cs}(k) \wedge E_{net}(k) \geq 0 \\
C_{on}^b(k)x(k) + D_{on}^b(k)u(k) + \Theta_{on}^b(k)\omega(k) & \text{for } \delta_{cs}(k) \wedge E_{net}(k) < 0
\end{cases}
\end{aligned}
\tag{20}
$$

The state space equations are switched according to the operation mode indicator δ_{cs} and directions of energy transactions with the UG, namely E_{net}. Further switching depends on energy exchange with the PES in the form of E_{bio} in the on-grid mode and the sum of E_{bio} and $z(k)$ in other modes. It should be noted that specific state space matrices change accordingly. Firstly, given $\delta_{cs} = 1$, the matrices marked with an appropriate subscript, such as system matrix A_{on}, correspond with equations originating from Subsection 2.1. Likewise, in off-grid and community mode, state space reflects the relationships introduced in Subsection 2.2. For instance, in on-grid mode, output, feed-through, and disturbances matrices alternate according to E_{net} between $C_{on}^s, D_{on}^s, \Theta_{on}^s$ indicating energy sales and $C_{on}^b, D_{on}^b, \Theta_{on}^b$ implying energy acquisition. Moreover, system, input, and disturbances matrices rotate between B_{on}^c, Ω_{on}^c and B_{on}^d, Ω_{on}^d in accordance with the PES charging and discharging related to E_{bio}. Furthermore, state $x(k)$, output $y(k)$, input $u(k)$ and disturbances vectors $\omega(k)$ are consecutively defined as:

$$
x(k) = \begin{bmatrix} E_{bat}(k) \\ E_{vbat}(k) \\ E_{rds}^1(k) \\ \vdots \\ E_{rds}^\tau(k) \end{bmatrix}
\qquad
y(k) = \begin{bmatrix} C_{net}(k) \\ C_{gen}(k) \\ E_{ib}(k) \\ E_{net}(k) \end{bmatrix}
$$

$$u(k) = \begin{bmatrix} E_{bio}(k) \\ E_{gen}(k) \\ E_{rdf}(k) \\ E_{rds}(k) \\ E_{ov}(k) \end{bmatrix} \qquad \omega(k) = \begin{bmatrix} \hat{E}_{res}(k) \\ \hat{E}_{d}(k) \\ z(k) \\ E_{net}^{req}(k) \\ E_{sd} \end{bmatrix}$$

Aside from said switching, output, feed-through, and disturbances matrices are also non-stationary due to energy price fluctuations.

3. Switched microgrid control system oriented towards economic optimisation

The authors employ a hybrid MPC to achieve sub-optimal control oriented towards economic factors regardless of operation mode. The predictive control approach allows the integration of the system model into the control law. This allows for taking into account the phenomena occurring in the microgrid, such as PES charging and discharging, and the non-stationarity resulting from energy market dynamics. Moreover, by re-configuring the control law according to the operation mode, the optimisation criteria can be better suited to given microgrid operation circumstances. What follows is that economic performance improves to a greater extent. A broader comparison of switched and classical control concerning microgrids is presented in [34].

3.1. Control system configuration

The microgrid operating in on-grid, off-grid, and community modes is relatively difficult to control using a unified approach. Depending on the operation conditions, the cost-optimality criteria change substantially. To mitigate this difficulty, authors employ a bi-level switched MPC. The individual modes or mode of operation correspond to a dedicated part of the control law. Figure 4 illustrates the control concept. The control law calculates control signals u based on an optimisation algorithm considering the mathematical model and some additional information. This information includes current state x, external connection status δ_{cs}, predictions concerning energy market $\hat{F}_s$ and $\hat{F}_b$, renewable energy generation $\hat{E}_{res}$, expected load $\hat{E}_d$ as well as community energy requests E_{net}^{req}. All predictions are carried N steps ahead in the receding horizon manner. The optimisation algorithm might require considerable time to find a feasible solution. For this reason, the control signals $u(k)$ executed at time kT_s result from optimisation performed utilising data measured at time $(k-1)T_s$, namely $x(k-1)$. This is illustrated in Figure 5. The system is also affected by the aggregate disturbances z associated with combined energy load and generation prediction errors.
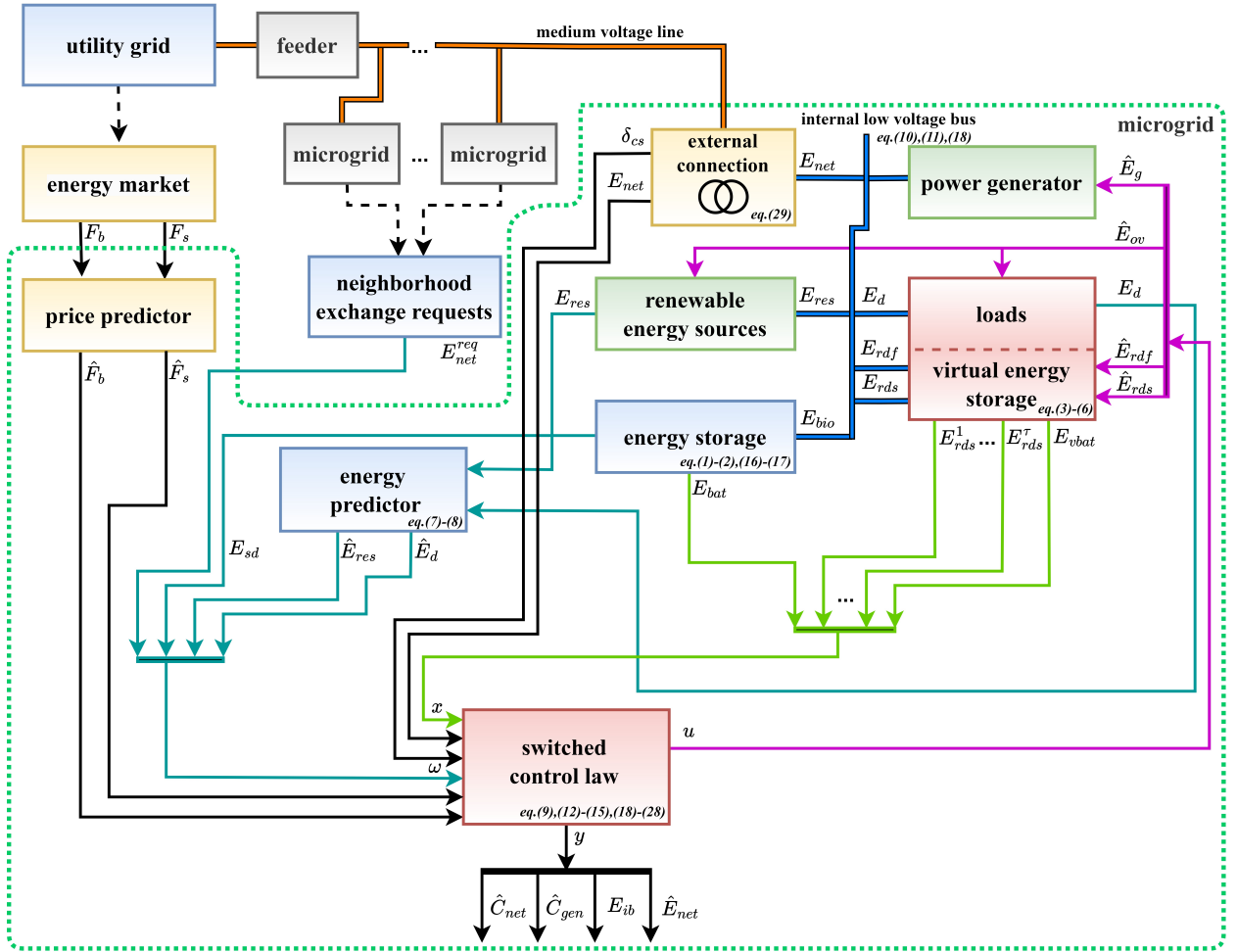
Figure 4: Diagram showing the flow of information between the microgrid, its environment and the control system.
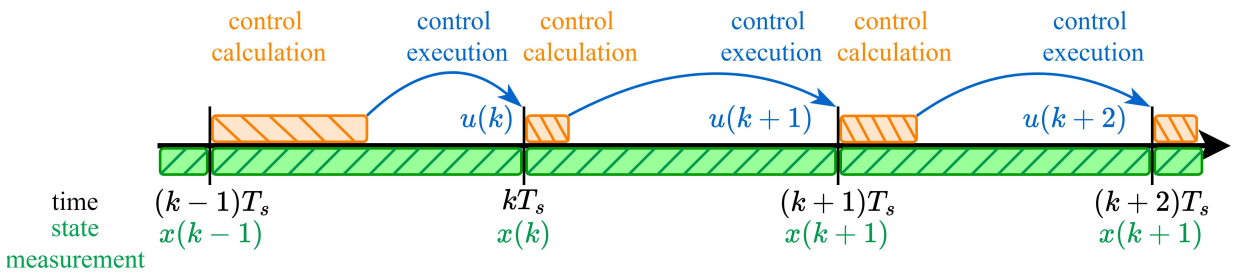
Figure 5: Diagram showing online calculation of control signals u taking computation and sampling time into consideration.

3.2. Associated optimisation problem

The cost function is considered the central element of any receding horizon algorithm. As previously mentioned, the authors opt for switched MPC. An appropriate cost function with fitting weighing matrices and reference values is chosen depending on the operation mode. Noteworthy, community and off-grid modes are similar enough to operate under the same controller configuration. Therefore, each cost function component switches only between two alternatives under the dictate of the operation mode. Regardless, cost J consists of two main parts. It should be noted that the weights presented represent a compromise

resulting from the priorities set by the authors. Nevertheless, the relevant elements of the weighting matrices have been subjected to sensitivity analysis. The first part, J_q, concerns the qualitative aspects of microgrid control focused on storage dynamics. The second part is denoted as J_e and reflects purely economic aspects of microgrid operation. Moreover, the terminal cost J_T assures that the state constraints are not violated. Introducing scaling coefficients s_q and s_e ensures proper proportions in the given operation mode. As illustrated in Equation 21, the qualitative component of cost function J comprises of terminal cost J_T, storage rate of change cost J_Δ and state cost J_x. As for the economics, the input associated cost J_u and the output bound cost J_y are considered.

$$J = s_q J_q + s_e J_e = \underbrace{s_q(J_T + J_\Delta + J_x)}_{\text{quality}} + \underbrace{s_e(J_u + J_y)}_{\text{economics}} \tag{21}$$

The scaling coefficients are also switched according to the connection status, as shown in Equation 22. The balance between J_e and J_q can be altered thanks to that. In turn, the controller can attach more importance to keeping the storage in check or lean toward better utilisation of cost reduction opportunities.

$$J = s_q J_q + s_e J_e = \begin{cases} s_q^{on} J_q + s_e^{on} J_e & \text{for } \delta_{cs} \\ s_q^{off} J_q + s_e^{off} J_e & \text{otherwise} \end{cases} \tag{22}$$

Equation 23 describes the switched terminal penalty, ensuring that VES and PES are kept within desirable levels. In this case, switching is limited to penalty matrices Q_T^{off} and Q_T^{on}. Given that the terminal penalty influences only the last prediction step N, associated weights are substantial. The non-zero weights appearing in matrices Q_T^{off} and Q_T^{on} refer to energy stores and should be jointly viewed with the reference values x_r^{off} and x_r^{on}. In on-grid mode, energy is readily available. So, accumulating cheap or renewable energy in PES is encouraged. Hence, the relatively high reference level of 85% and large weight are responsible for its tracking. In off-grid mode, the weight is less because energy cannot be bought from the UG. However, it is still important to encourage the system to accumulate renewable energy and not discharge the PES deeply. Regardless of the mode, the reference value of the VES is zero because it is desirable to equalise deficits and surpluses at the end of the prediction horizon. For the same reason, such large weight values are adopted. Due to the operating conditions, DM is extensively used in off-grid mode, and an even more significant penalty is needed. Scaling matrix s_x, ensuring the signal resolution from zero to one, is also included. Scaling factors for respective state variables are calculated as the inverted range between their minimal and maximal values. The remaining elements of all four matrices are zero because the corresponding signals are irrelevant and stem from DSR implementation

$$J_T = \begin{cases} \|s_x Q_T^{on}(x_N - x_r^{on})\|_1 & \text{for } \delta_{cs} \\ \|s_x Q_T^{off}(x_N - x_r^{off})\|_1 & \text{otherwise} \end{cases} \tag{23}$$

The weighting matrices Q_T^{off} and Q_T^{on} as well as reference values x_r are defined as follows:

$$Q_T^{off} = \begin{bmatrix} 27.5 & & & & \\ & 1000 & & & \\ & & 0 & & \\ & & & \ddots & \\ & & & & 0 \end{bmatrix} \quad Q_T^{on} = \begin{bmatrix} 90 & & & & \\ & 500 & & & \\ & & 0 & & \\ & & & \ddots & \\ & & & & 0 \end{bmatrix}$$

$$x_r^{off} = \begin{bmatrix} 0.75\overline{E}_{bat} \\ 0 \\ \vdots \\ 0 \end{bmatrix} \quad x_r^{on} = \begin{bmatrix} 0.85\overline{E}_{bat} \\ 0 \\ \vdots \\ 0 \end{bmatrix}$$

Subsequently, authors find it necessary to include additional factors in the cost function to mitigate rapid PES level fluctuations. Therefore, the state rate of change cost J_Δ is introduced and switched according

to the connection status δ_{cs}. Notably, only the PES rate of change is penalised. Proper scaling is ensured using the matrix s_{dx}.

$$J_\Delta = \begin{cases} \sum_{i=k}^{k+N} \|s_{dx}Q_\Delta^{on}(x_i - x_{i-1})\|_1 & \text{for } \delta_{cs} \\ \sum_{i=k}^{k+N} \|s_{dx}Q_\Delta^{off}(x_i - x_{i-1})\|_1 & \text{otherwise} \end{cases} \tag{24}$$

The penalty associated with the PES state of charge is aimed at forcing the control system to utilise other means of energy flow control, namely demand shifting and power generator. Fluctuations in VES are, therefore, acceptable and welcome. That is why the corresponding elements of the matrices Q_Δ^{off} and Q_Δ^{on} equal zero. Strong PES level fluctuations in off-grid and community modes are more likely because the imbalance is equalised using PES instead of UG. A heavier penalty is applied to mitigate that and maintain an acceptable PES level.

$$Q_\Delta^{off} = \begin{bmatrix} 4 & & & \\ & 0 & & \\ & & \ddots & \\ & & & 0 \end{bmatrix} \qquad Q_\Delta^{on} = \begin{bmatrix} 1 & & & \\ & 0 & & \\ & & \ddots & \\ & & & 0 \end{bmatrix}$$

Furthermore, the last component of J_q is the base penalty J_x, which is responsible for reference state tracking over the entire horizon.

$$J_x = \begin{cases} \sum_{i=k}^{k+N} \|s_x Q_x^{on}(x_i - x_r^{on})\|_1 & \text{for } \delta_{cs} \\ \sum_{i=k}^{k+N} \|s_x Q_x^{off}(x_i - x_r^{off})\|_1 & \text{otherwise} \end{cases} \tag{25}$$

Weighting matrices Q_x^{on} and Q_x^{off} are complementary to the pair Q_T^{off} and Q_T^{on} and the same reference signals are used. However, the relationship between the weights dedicated to the two energy stores differs. In off-grid mode, keeping the PES from deep discharge is deemed more important than equalising the energy deficit or surplus stored in the VES. The opposite applies in on-grid mode when energy from the UG can easily influence the PES level. Ensuring the user gets a fair energy allocation is more important in such a case. Therefore, the weight for VES is greater.

$$Q_x^{off} = \begin{bmatrix} 2.8 & & & & \\ & 1.5 & & & \\ & & 0 & & \\ & & & \ddots & \\ & & & & 0 \end{bmatrix} \qquad Q_x^{on} = \begin{bmatrix} 2.1 & & & & \\ & 2.5 & & & \\ & & 0 & & \\ & & & \ddots & \\ & & & & 0 \end{bmatrix}$$

The economically oriented part of cost function J_e has a bipartite structure. Firstly, the input-associated part J_u remains the same regardless of the operation mode. It consists of the weighted sum of the input vector u_i multiplied by the weight matrix R as described in Equation 26.

$$J_u = \sum_{i=k}^{k+N} Ru_i \tag{26}$$

Numerical values of individual weights included in R are chosen based on cost. The weighting coefficient associated with the energy exchange E_{bio} is selected based on two factors. These are the rounded product of normalised energy price over two years and the average percentage loss of energy due to the efficiency η of the PES. To encourage the utilisation of VES, authors chose twofold and fourfold smaller penalties for fast and slow load reduction, respectively. A relatively large penalty is selected for using the overflow mechanism E_{ov}. This ensures that the solution will only feature non-zero E_{ov} when necessary. Auxiliary generator usage is penalised in the output-associated component of the cost function. Hence, the respective weight contained

in R equals zero.

$$R = \begin{bmatrix} 0.006 & & & & \\ & 0 & & & \\ & & 0.003 & & \\ & & & 0.0015 & \\ & & & & 1000 \end{bmatrix}$$

Output-associated cost J_y integrates two main cost or income sources: on-site auxiliary power generation and energy transactions with the UG. As seen from Equation 27, this part of the cost function also holds regardless of the operation mode. Due to the intended profit maximisation, y_i features a negative sign. Assuming that positive values of J_y indicate profit and negative indicate loss, the minimised combined cost J is reduced as the presumptive profit increases.

$$J_y = \sum_{i=k}^{k+N} -S y_i \tag{27}$$

Moreover, due to only two first elements of the output vector being cost-associated, the weight matrix S has only two non-zero values on its diagonal. Importantly, those values are set to one given the already appropriately scaled generator cost and energy transactions measures C_{gen} and C_{net}. As a result, both J_y and J_u are expressed in monetary form.

$$S = \begin{bmatrix} 1 & & & \\ & 1 & & \\ & & 0 & \\ & & & 0 \end{bmatrix}$$

Finally, the optimisation problem contains state, output and lower input bounds. Varying upper input constraints are also present. Importantly, the fast DM E_{rdf} may only cover a percentage of current demand and should not be performed blindly. Authors assume that fast load reduction can decrease or increase the load by only up to a certain degree of expected load. Therefore, the varying upper constraint derived as a percentage r_d of predicted energy demand $\hat{E}_d$ is introduced. Problem 28 is solved assuming the negligible influence of immeasurable disturbances and constant operation mode over the prediction horizon N. Those assumptions are made due to the immeasurable nature of energy, pricing-related disturbances, and the uncertain future connection status. According to the classification presented in [47], Problem 28 can be formulated as a Mixed Integer Linear Program (MILP). Many well-established methods exist for solving a MILP problem built on the widely used MLD representation [47]. The resulting control signal set u_i through u_{i+N} describes the optimal control sequence over prediction horizon N. It is the solution of the optimisation problem at the given time step k. The first control vector from the set, u_i is then applied to the microgrid as $u(k)$.

$$\begin{aligned} &\underset{u_i,\dots,u_{i+N}}{\text{minimise}} \quad J \\ &\text{subject to} \\ &\qquad \underline{x} \le x_i \le \overline{x} \\ &\qquad \underline{u} \le u_i \le \overline{u}_i \\ &\qquad \underline{y} \le y_i \le \overline{y} \\ &\qquad z_i, \dots, z_{i+N} = 0 \\ &\qquad \overline{u}_i = \begin{bmatrix} \overline{E}_{bio} & \overline{E}_{gen} & r_d \hat{E}_d(k+i) & \overline{E}_{rds} & \overline{E}_{ov} \end{bmatrix}^\mathsf{T} \\ &\qquad \text{Expression 20 holds for each } x_i \text{ and } y_i. \end{aligned} \tag{28}$$

4. Testing methodology

The developed microgrid hybrid model and switched control system are implemented in Matlab. The environment is enhanced with YALMIP [48], and the optimisation problem is solved online using Gurobi Optimizer [49]. Table 2 lists various model and controller parameters. It should be noted that the notation using overline and underline is used to denote the constraints. Overline indicates an upper bound, and underline indicates a lower bound for a given variable. The PES capacity E_{bat} of 1000 kWh is selected to ensure four to five hours of energy supply in case of the full load of 200 kW. The PES also aims to ensure between two and three hours of energy reception in case of low PES level and full rated power of renewable generation E_{res}. Moreover, an 85% roundabout PES efficiency is chosen, which is typical for a battery storage system according to [50] and [51]. Additional constraints concerning the PES level rate of change ΔE_{bat} are introduced to facilitate limited charge and discharge capabilities. The constraints must be respected despite operation mode changes and imbalance suppression using PES in off-grid and community modes. At the same time, the maximal VES capacity E_{vbat} is set as half of the permitted PES level in both directions. The maximal amount of energy shifted must be sufficient to influence the energy balance significantly. The maximal slow and fast demand reduction or increase are set to 20% of maximal demand and 5% of actual demand, respectively. Consumers with short response times are considered to include, for example, heating or ventilation equipment. Manufacturing processes or electric vehicles are considered potentially subject to slow management. Consequently, the first group can react quickly, but the potential amount of energy is much smaller than in the second group, which requires a long preparation. The rated power of the auxiliary generator of 100 kW is adopted. The microgrid can exchange up to 300 kW of energy every hour with the UG. Further, 100 kW can be exchanged with the community regardless of the direction of energy flow. This means that the amount of energy drawn from the UG cannot be entirely replaced by the generator in off-grid mode. By looking at the historical energy pricing data [44], a maximal energy price of 0.5 € per kilowatt-hour is adopted. The prediction horizon is set at eleven steps, and the sampling time is one hour. Appropriate PES capacity, power and permissible state of charge range choice is vital. The expected operating time in on-grid and off-grid modes must be considered when making that selection. The selection of these and other relevant microgrid parameters is usually a trade-off between the costs and expected benefits. However, the authors focus on controlling a microgrid with an already established infrastructure. The transmission line rated power is assumed as $\overline{\overline{S}}_{net}$ and the minimal value of the power factor as $\underline{PF}$. Consequently, the upper energy exchange bound $\overline{E}_{net}$ and lower bound $\underline{E}_{net}$ are implied by Equation 29.

$$\overline{E}_{net} = -\underline{E}_{net} = T_s \overline{S}_{net} \underline{PF} \tag{29}$$

Firstly the authors intend to check the ability of the system to keep all variables in desirable subspace and act logically. A simple fictional disturbance scenario and a scenario considered a baseline are used for the analysis. Secondly, the influence of the prediction horizon N length on the chosen indices is considered. Thirdly, the sensitivity concerning chosen weight matrices is scrutinised based on the cost J. Then, the influence of immeasurable disturbance z is analysed by introducing a chosen subset of expected values and standard deviation. The same set of four random number generator seeds is kept during testing. Lastly, the authors intend to analyze the influence of load preponing and postponing implemented through the proposed VES. At the same time, the performance of the proposed control system under varying connection conditions and initial conditions is studied. The evaluation shall be based on criteria selected from among the following:

- total energy cost $\sum C_{net}$ over the evaluated time horizon of ninety-six hours

- total auxiliary generator usage cost $\sum C_{gen}$

- total energy lost due to foreseen and unforeseen PES overflow $\sum E_{ov}$

- average PES level mean(E_{bat})

- average VES level mean(E_{vbat})

Table 2
optimisation problem parameters, tuning weights and constraints.

Parameter	Value	Unit	Parameter	Value	Unit
$\overline{E}_{bat}$	1000	kWh	$\underline{E}_{bat}$	100	kWh
$\Delta \overline{E}_{bat}$	122	kWh	$\Delta \underline{E}_{bat}$	-440	kWh
$\overline{E}_{bio}$	250	kWh	$\underline{E}_{bio}$	-200	kWh
$\overline{E}_{vbat}$	500	kWh	$\underline{E}_{vbat}$	-500	kWh
$\overline{E}_{rds}$	40	kWh	$\underline{E}_{rds}$	-40	kWh
$\overline{E}_{rdf}$	10	kWh	$\underline{E}_{rdf}$	-10	kWh
$\overline{E}_{d}$	200	kWh	$\underline{E}_{d}$	0	kWh
$\overline{E}_{res}$	400	kWh	$\underline{E}_{res}$	0	kWh
$\overline{E}_{gen}$	100	kWh	$\underline{E}_{gen}$	0	kWh
$\overline{E}_{ov}$	300	kWh	$\underline{E}_{ov}$	-300	kWh
$\overline{E}_{net}$	300	kWh	$\underline{E}_{net}$	-300	kWh
$\overline{E}_{net}^{req}$	100	kWh	$\underline{E}_{net}^{req}$	-100	kWh
$\overline{F}_{net}$	0.5	€/kWh	$\underline{F}_{net}$	0	€/kWh
$\overline{S}_{net}$	400	kVA	$\underline{PF}$	0.75	-
η_c	0.85	-	η_d	0.85	-
N	11	T_s	T_s	1	h
r_d	0.05	-	F_{gen}	0.40	€/kWh
E_{sd}	2	kWh			
s_e^{on}	3.15	-	s_q^{on}	1	-
s_e^{off}	1.05	-	s_q^{off}	1	-
s_x	$\mathrm{diag}\left(\begin{bmatrix} 900 & 1000 & 80 & \ldots & 80 \end{bmatrix}\right)^{-1}$				$1/kWh$
$s_{\Delta x}$	$\mathrm{diag}\left(\begin{bmatrix} 562^{-1} & 0 & \ldots & 0 \end{bmatrix}\right)$				$1/kWh$

- average computation time $\mathrm{mean}(t_{clc})$

At this point, one should also mention that calculation time t_{clc} refers to optimisation times achieved using a particular workstation. It is equipped with an AMD 5950x CPU and 64 GB of RAM. It is presumed that the simulated microgrid can reduce the output of renewable energy sources in case of PES overflow, regardless of control signals.

The authors intend to use as much factual data as possible. Renewable energy generation data and load normalised data used during testing were acquired from a microgrid localised in the West Pomeranian region in Poland and re-scaled accordingly. Furthermore, time-coupled energy price data are sourced from [44]. A 20% spread between purchase and sales price is assumed. Prediction inaccuracy in the form of $z(k)$ is generated as a random variable with zero expected value $EV(z)$ and a standard deviation of five. The connection scenario consists of twenty-four hours in community mode, after which the microgrid operates in the off-grid mode for another twenty-four hours. Then, the rest of the simulation is spent in on-grid mode. Over the first twenty-four hours, the community energy influx builds up, then gradually changes into community demand and returns to zero. This scenario ensures the equality of energy supplied and received from the community while sufficiently complicating the control problem at a given time step. Figure 6 illustrates the scenario. Table 3 consists of essential measures describing energy-related signals. Noteworthy, renewable energy influx is similar compared to the overall load. The scenario also reflects the non-consistency of renewable energy sources. Moreover, the aggregate disturbance z indicates that the simulated predictor tends to undervalue the expected load and demand. Energy prices are characterised by significant deviations
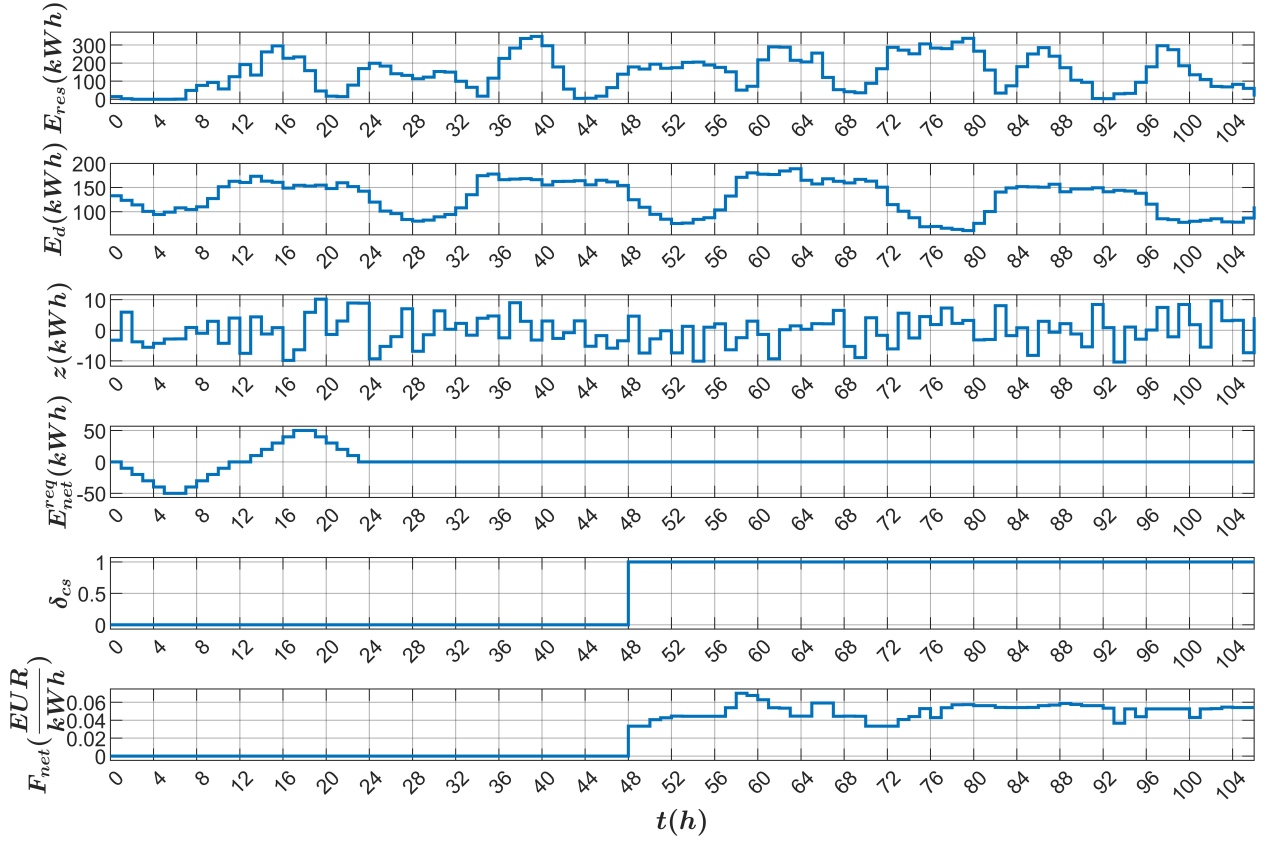
Figure 6: Primary simulation scenario consisting of renewable energy generation, energy demand, immeasurable disturbance $z(k)$ and pricing used during testing. In off-grid and community mode, energy price is zeroed.

Table 3
Selection of indices of disturbance signals making up the disturbance scenario considered during testing.

Index	Value	Unit
$\sum z$	-14.91	kWh
$\sum E_{res}$	1388.58	kWh
$\sum E_d$	1376.67	kWh

from the mean value that the controller may exploit. Such a combination is then used as a baseline scenario. Certain elements, such as disturbances z or initial conditions, are modified according to the given testing routine. The only exception is the first test, which assumes no disturbances and no energy exchange with the community. Price, demand, and generation scenarios are shown in Figure 6.

5. Results

5.1. Initial testing utilising simplified and primary scenarios

The first test involves a fictional demand and generation scenario with no disturbances. The difference between demand and generation is set as a rectangular waveform. Figure 7 presents obtained system responses over ninety-six hours in a mixed operation mode scenario. All signals are normalised to the form of x^n using the maximum value of a given signal obtained during the simulation as shown in Equation 30.

$$x^n(k) = \frac{x(k)}{\max_k(|x(k)|)} \tag{30}$$

Regardless of operation mode, the PES is charged with renewable energy whenever possible. The VES dampens the effect of energy deficiency and surplus in off-grid mode. Moreover, in on-grid mode, the VES also allows for greater energy acquisition and sale at a favourable price. As intended, fast DM E_{rdf} is used mainly to mitigate abrupt changes in energy balance. Conversely, E_{rds}^8 is responsible for countering long-term effects and profitable energy exchange in on-grid mode. Auxiliary generator E_{gen} is used only when the PES is in danger of being deeply discharged. The authors find the results of this simplified test to be in line with expectations. Figure 8 summarises simulation results for primary scenario. Noteworthy, the controller uses
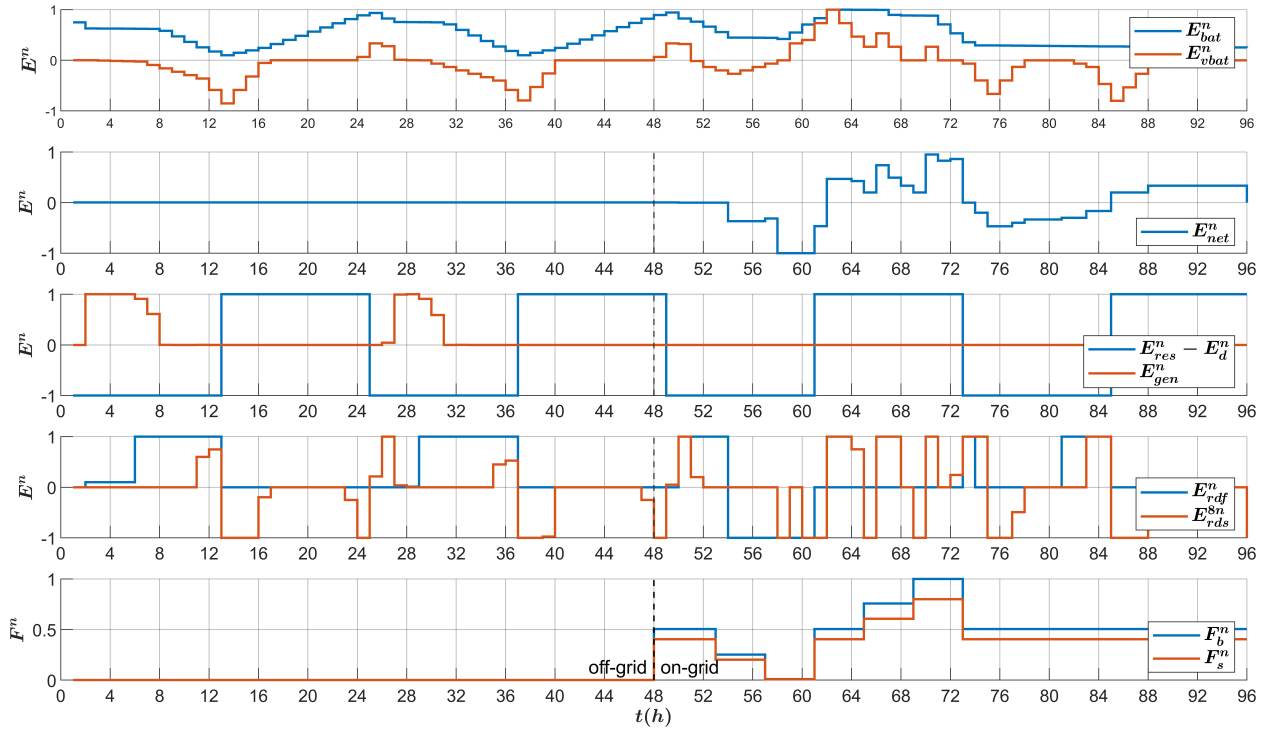

Figure 7: Selected normalised state, input, and output signals during ninety-six hours of simulation assuming no prediction error and the difference between demand and generation expressed as a rectangular waveform.

the VES to mitigate the impact of volatile energy balance on the PES level. This includes fluctuations in the energy supply and demand relationship and the energy exchange with the community. In addition, the VES is utilised to reduce the degree of auxiliary generator usage. Thanks to the VES, energy is consumed in advance during low-price periods. Simultaneously, demand is postponed during high-price periods to achieve economic benefits by making more energy available for sale. Parallels to the simplified scenario can be drawn.
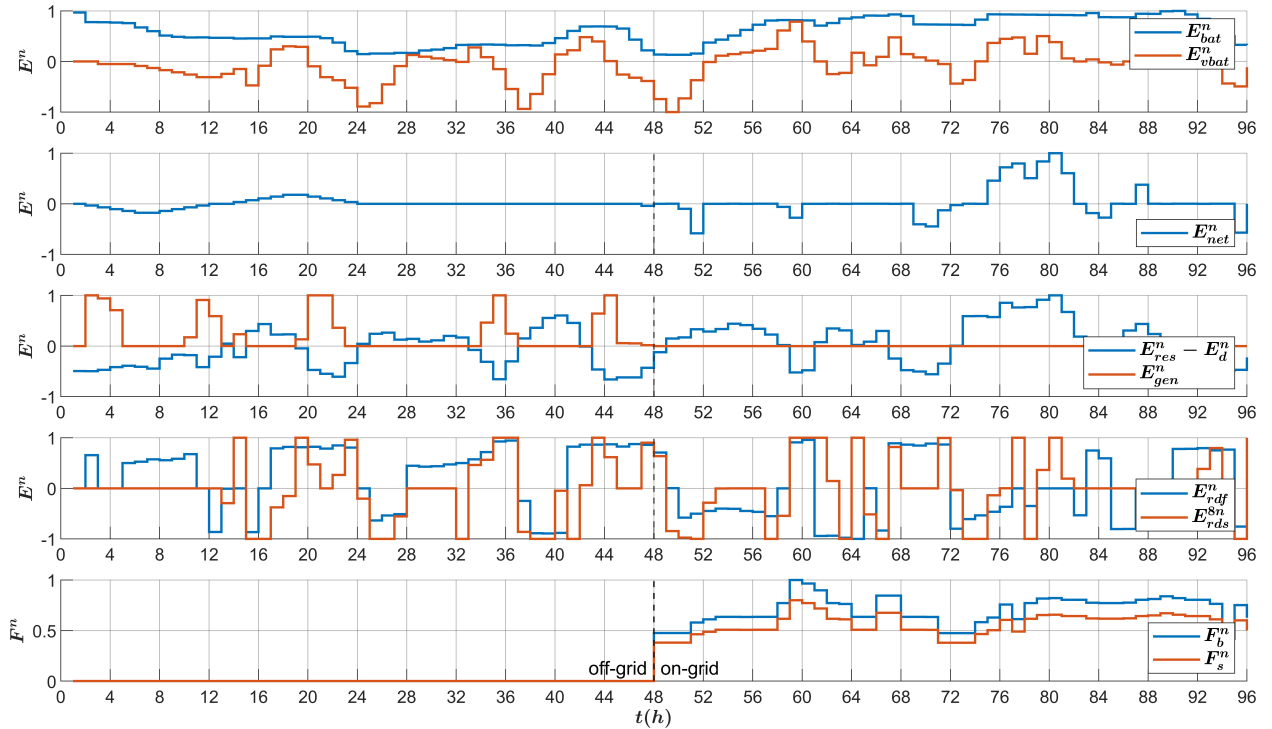
Figure 8: Selected normalised state, input and output signals during ninety-six hours of simulation utilizing primary simulation scenario.

5.2. Study of the effect of prediction horizon length on control quality

Considering the usage of MPC, it is necessary to check how the values of the control quality indices adopted for the tests change. Table 4 summarises selected control quality indices for different horizon lengths. Based on the data collected in Table 4, the prediction horizon of eleven time-steps ensures the lowest value of optimisation-associated cost J. In addition, the amount of energy stored in PES increases with horizon length. Conversely, the amount of energy lost through overflow shows no clear dependence on N. The operation cost expressed in EUR decreases with horizon length although better economic performance is ransomed by the increase in optimisation time. Precisely because of the overly lengthy calculation time t_{clc}, prediction horizons greater than eleven are not considered. This is due to the adopted testing methodology requiring multiple simulations.

Table 4
Selection of performance indices and calculation time in relation to prediction horizon length.

Index	N = 5	N = 7	N = 9	N = 11	N = 12	N = 13	Unit
mean(J)	51.03	50.14	54.98	40.48	44.92	46.47	-
mean(t_{clc})	6.97	15.93	62.22	143.99	176.94	198.65	s
mean(E_{ov})	4.00	2.00	2.00	2.00	2.00	2.00	kWh
mean(E_{bat})	254.80	333.07	358.77	463.71	467.58	460.98	kWh
$\sum C_{net} + \sum C_{gen}$	485.03	469.29	443.99	400.78	385.91	371.26	€

5.3. The sensitivity of optimisation problem weighting matrices

An important issue in selecting cost function weights is to examine the sensitivity of the chosen configuration. The authors scrutinise how an m-percent change in a given weight influences the optimisation-related cost J. The difference between the value of J with unchanged weights and the cost obtained using modified weight matrices is marked with ΔJ. The obtained percentage change of the relation between J and ΔJ is referred to as sensitivity ζ_m and is described using Equation 31.

$$\zeta_m = \frac{\Delta J}{J_0} 100\% \tag{31}$$

Sensitivity is tested only for non-zero weights, which may have to be modified for a model with other parameters. Individual weighting matrices such as Q contain the weights corresponding to each signal on their diagonals. In Table 5, referring to the weight placed in the first column and the first row of the Q matrix, the notation $q(1,1)$ is used. Due to the switched control law, a separate analysis is carried out for each mode of operation. Table 5 presents the sensitivity-related data collected in off-grid mode. As can be seen, the overall sensitivity is relatively low. The most significant changes occur when weights $q(1,1)$ and $s(2,2)$ change. The first of those weights is associated with the state of charge of the PES. In the case of off-grid operation, a change in the value of said weight can cause large changes. This is due to the difficulty of obtaining energy. In contrast, $s(2,2)$ penalises the regulator for using the auxiliary generator, mainly used in times of energy shortage. Its operation is costly, so changing the corresponding weight has a distinct effect.

Table 6 shows that the sensitivity in the on-grid mode is much higher but only for certain weights. Significant changes occur when modifying $q(2,2)$ associated with PES. This is understandable, given that it indirectly determines the possibility of using the PES for energy market operations. Identical conclusions can be drawn regarding $q_T(1,1)$. Weights $r(1,1)$ and $s(1,1)$ are responsible for energy exchange with the UG. Their configuration encourages or discourages the control system from taking advantage of the market situation.

Table 5
Sensitivity of the weight matrices of the optimisation problem in off-grid mode.

weight	m=-5%	m=-2%	m=-1%	m=+1%	m=+2%	m=+5%	Unit
$q(1,1)$	-1.3223	-0.8277	-0.6597	0.1681	0.3393	1.5046	%
$q(2,2)$	-0.0198	-0.0219	-0.0125	0.0125	0.0295	-0.3745	%
$q_\Delta(1,1)$	-0.1982	-0.0793	-0.0396	-0.4519	-0.4122	0.2147	%
$q_T(1,1)$	-0.8599	-0.3439	-0.1720	0.1720	0.3439	0.8599	%
$q_T(2,2)$	0.0000	0.0000	0.0000	0.0000	0.0000	0.0000	%
$r(1,1)$	-0.1359	-0.5461	-0.0272	0.0272	0.0544	0.1359	%
$r(3,3)$	-0.4201	-0.4940	-0.4928	0.0012	0.0024	0.0092	%
$r(4,4)$	-0.0039	-0.0016	-0.0008	0.0008	0.0016	0.0039	%
$s(1,1)$	0.0000	0.0000	0.0000	0.0000	0.0000	0.0000	%
$s(2,2)$	-2.8930	-1.1572	-0.5786	0.5786	1.1572	2.8930	%

Table 6
Sensitivity of the weight matrices of the optimisation problem in on-grid mode.

weight	m=-5%	m=-2%	m=-1%	m=+1%	m=+2%	m=+5%	Unit
$q(1,1)$	-10.1222	-12.1692	0.6858	-0.6514	-1.2629	27.5560	%
$q(2,2)$	-2.8247	0.1274	0.0444	-0.0831	-0.0317	-0.1505	%
$q_\Delta(1,1)$	0.3158	0.1179	0.0625	-0.0394	-0.0927	-0.3319	%
$q_T(1,1)$	19.9376	8.0447	4.0015	-3.8445	23.8552	27.3926	%
$q_T(2,2)$	-0.0044	0.0001	-0.0028	-0.0039	0.0002	0.0040	%
$r(1,1)$	32.3561	31.1063	0.4085	-0.4024	-0.8094	-81.9303	%
$r(3,3)$	0.2172	0.0716	0.0563	-0.0224	-0.0478	-0.0743	%
$r(4,4)$	0.0613	0.0249	0.0144	-0.0169	-0.0262	-0.0632	%
$s(1,1)$	11.3404	18.9523	-5.8852	6.2198	-1.2045	61.6756	%
$s(2,2)$	-0.0002	0.0005	-0.0040	-0.0002	-0.0060	-0.0005	%

5.4. Study of the influence of energy demand and renewable generation predictions accuracy on microgrid control performance

The authors evaluated the microgrid operation performance to determine the importance of accurate energy demand and generation forecasting while changing the disturbance distribution between Gaussian and uniform. The distribution parameters that are also subject to change are the expected value and standard deviation z. The seed of the random number generator remained always the same within a single series of tests. This approach is chosen to obtain simulation results independent of the specific disturbance sample. The entire test series is repeated four times with different random number generator seeds for each disturbance distribution. The final results are averages of the four series. As part of each series of tests, the following properties of prediction error distribution are modified:

- the expected value takes the values in the range from -10 to 10 kWh with intervals of 5 kWh

- the standard deviation takes the values from 0 to 20 kWh with intervals of 5 kWh

and the performance criteria values mentioned in Section 4 collected. Figures 9-12 show the values of selected indices in relation to standard deviation and expected value of disturbances $z(k)$ for both normal and uniform distributions. Figure 9 shows the total cost, Figure 10 the average PES level, Figure 11 the average VES level, and Figure 12 the energy lost due to PES overflow.
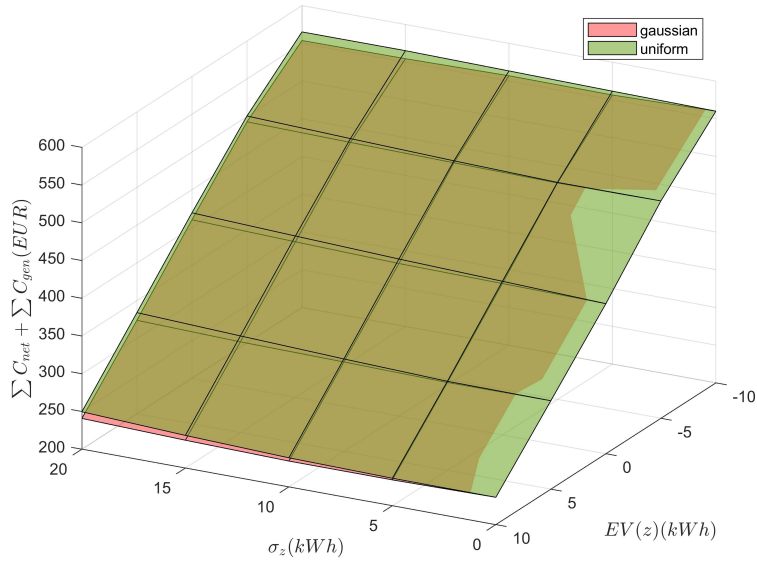
Figure 9: Microgrid operation costs in relation to standard deviation and expected value of disturbances $z(k)$.
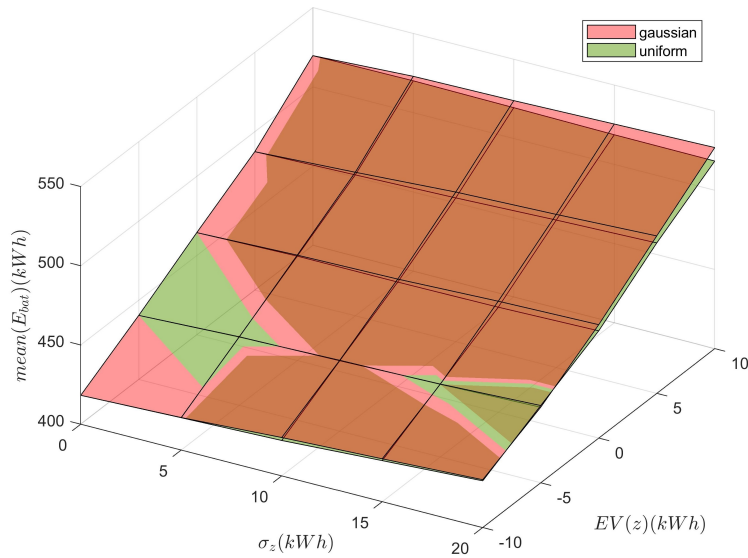

Figure 10: Average PES level in relation to standard deviation and expected value of disturbances $z(k)$.

As seen by looking at Figure 9, total operation cost decreases with the expected value of z and decreases slightly with the increase of the standard deviation. Such an outcome is understandable given that the overestimation of $z(k)$ encourages more aggressive utilisation of available energy. Simultaneously, it discourages auxiliary generator usage. On the contrary, underestimation of $z(k)$ concedes restrained usage of stored resources but induces unnecessary generator use. The average PES level, visible in Figure 10, is characterised by the same dynamics as operation costs. By feeding the control law exaggerated estimates of surplus energy, more energy is stored. Additionally, greater values of δ_z also increase the average E_{bat}. The opposite situation applies to VES, as shown in Figure 11. Overestimation of disturbances leads to a greater degree of load reduction. In contrast, the amount of energy lost by PES overflow shown in Figure 12 is
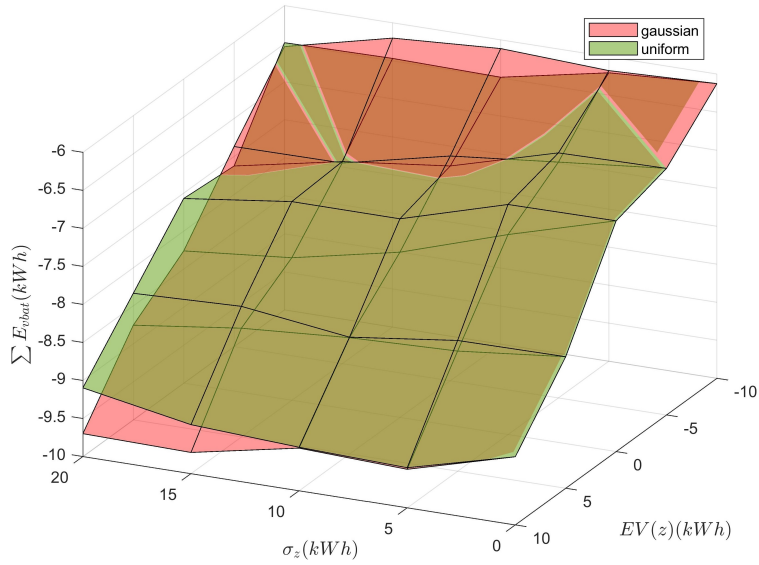
Figure 11: Average VES level in relation to standard deviation and expected value of disturbances $z(k)$.
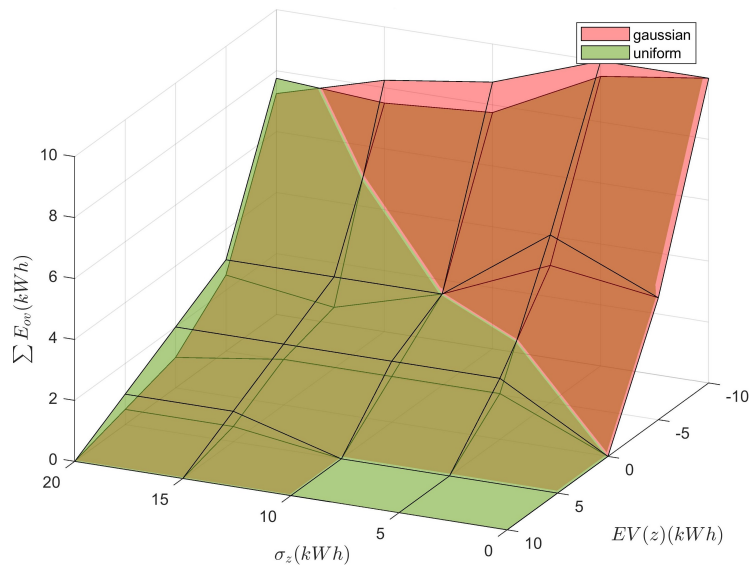

Figure 12: Energy lost due to overflow in relation to standard deviation and expected value of disturbances $z(k)$.

inversely proportional to the expected value of z. This is understandable, given the risk of underestimating the amount of energy in the system. What is important is that differences between distributions are negligible.

5.5. Analysis of the influence of the introduction of load preponing and postponing capabilities in microgrid control system

Other authors have already discussed the advantages of the introduction of a VES. This work explores the various possibilities for managing demand regarding time and energy volume. The influence of introducing the proposed management scheme is scrutinised by comparing system performance with different demand-shaping capabilities. Load preponing, postponing, and bidirectional operation are considered. To broaden the analysed scope, the authors trial all control systems in changing initial conditions and proportions between on-grid and off-grid/community modes. This is achieved by:

- introducing initial PES level in the range from 300 to 900 kWh with intervals of 150 kWh

- introduction of the variable ratio of on-grid and off-grid operation time during the 96-hour-long simulation. The simulation always starts in off-grid mode, but the time of switching to on-grid operation t_s varies from hour 1 to 81 with intervals of 20 hours.

Table 7 shows a summary of selected measures of control quality depending on the type of VES used.

Firstly, looking at the data in Table 7, one can spot that load postponing leads to the least income from energy sales while other variants achieve similar gains. Nonetheless, the bidirectional VES achieves the best cost performance regarding auxiliary generation. The highest average state of charge is associated with preponing alone, and the bidirectional battery provides the lowest state of charge. As far as the level of VES is concerned, its average, as expected, lies close to zero for the bidirectional VES. These average values also correspond to the sign of the permissible values in the other cases. The total energy lost due to PES overflow is negligible, but the lowest losses are recorded using load preponing exclusively. Compared to the system without the VES, bidirectional management ensures significant operational cost reduction and an average degree of energy shortage. At the same time, it should be noted that the average amount of energy stored in PES is lower and the amount of energy lost due to PES overflow is more significant. Figures 13-16 illustrate the dependence of selected indices on the initial PES state of charge and the transition time from off-grid to on-grid mode for different VES types. Figure 13 shows the total cost, Figure 14 the average PES level, Figure 15 the average VES level, and Figure 16 the energy lost due to PES overflow.
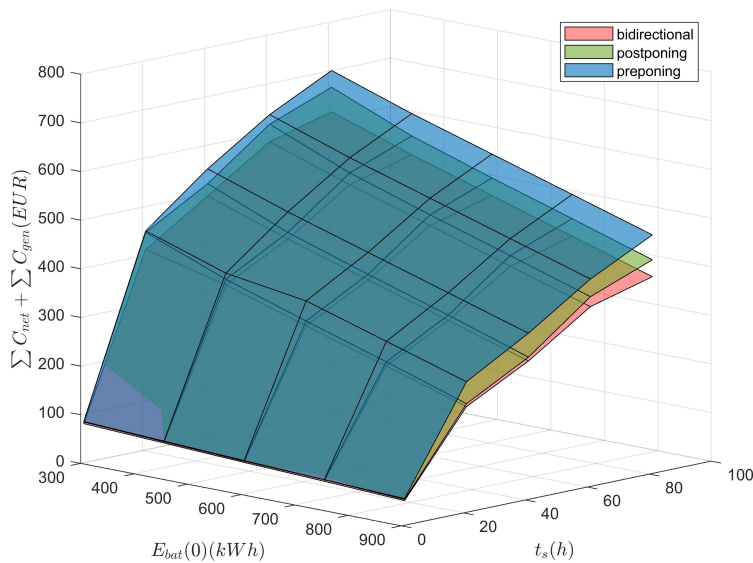

Figure 13: Dependence of the total cost of microgrid operation on the initial PES state of charge and the transition time from off-grid to on-grid mode for different VES types

Table 7

Comparison of selected performance and cost measures in relation to different types of DM utilizing VES and devoid of it.

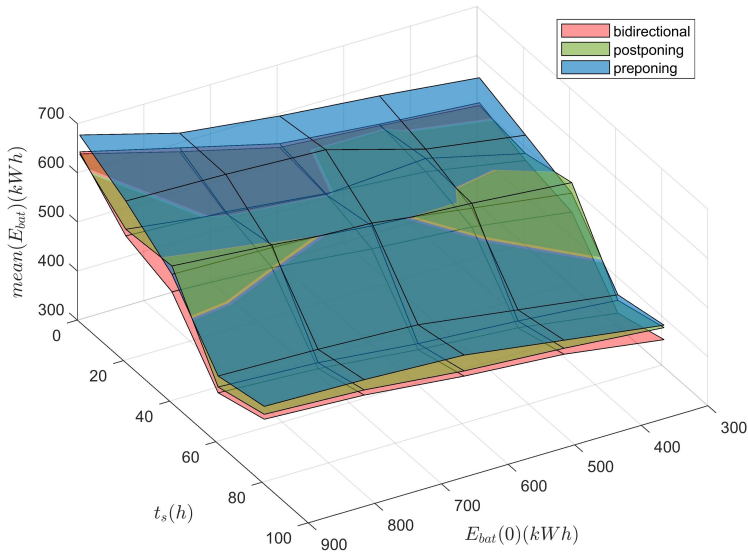| Measure	preponing	postponing	bidirectional	no VES	Unit
mean($\sum C_{net}$)	-6.07	-2.43	-6.01	-4.717	€
mean($\sum C_{gen}$)	405.57	371.89	356.48	425.28	€
mean(E_{bat})	515.18	486.89	470.17	538.28	kWh
mean(E_{vbat})	25.52	-24.49	-0.73	0.00	kWh
mean($\sum(E_{ov})$)	1.20	2.00	2.00	0.80	kWh
mean($\sum(E_{blck})$)	0.68	1.00	0.76	1.20	kWh

Figure 14: Dependence of the average PES level on the initial PES state of charge and the transition time from off-grid to on-grid mode for different VES types

As Figure 13 indicates, the lowest operation cost is obtained for high initial charge states and pure on-grid operation regardless of the VES variant. At the same time, operation costs rise with the extension of off-grid operations. Moreover, the bidirectional VES ensures the lowest operation cost regardless of the scenario. The average state of charge of the PES as the off-grid operating time increases and its initial charge decreases, as shown in Figure 14. In contrast, according to Figure 15, the average state of charge of the VES does not depend on the initial state of the PES. Moreover, the state of charge rises noticeably when operating mostly in off-grid mode. Although negligible, the amount of lost energy depends on off-grid operation time, as depicted in Figure 16. This is understandable, given the greater risk of overflow in the PES when there is no possibility of selling excess energy.
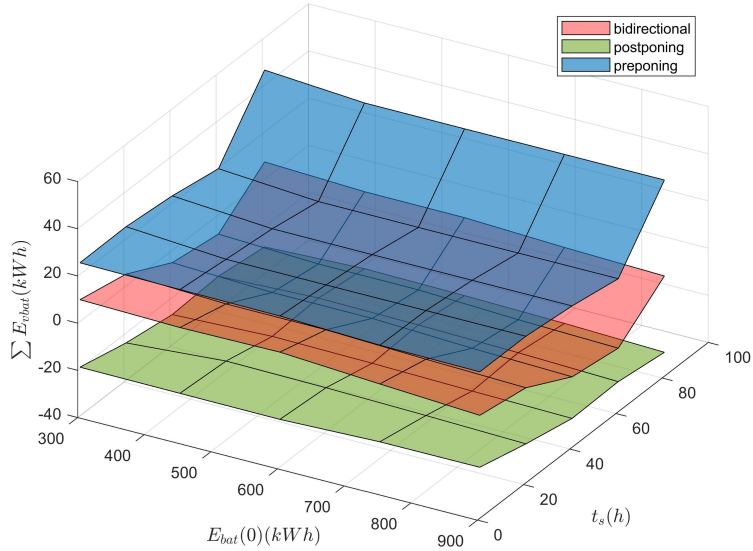
Figure 15: Dependence of the average VES level on the initial PES state of charge and the transition time from off-grid to on-grid mode for different VES types
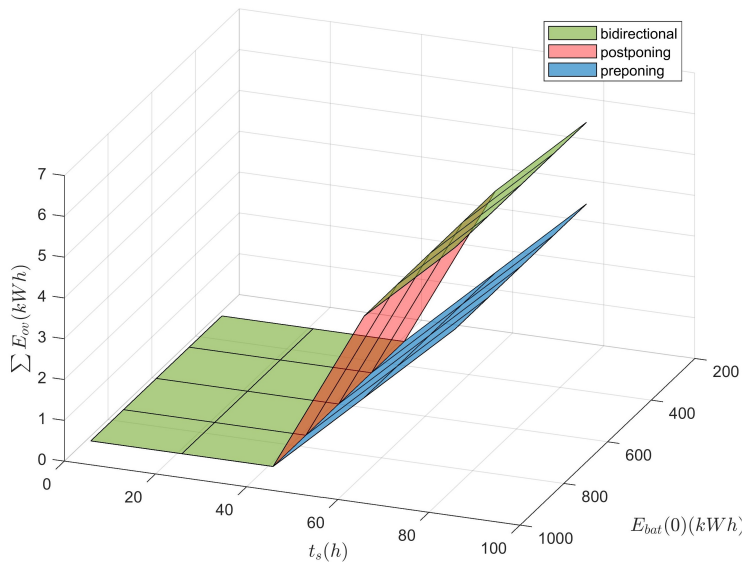

Figure 16: Dependence of the energy lost to PES overflow on the initial PES state of charge and the transition time from off-grid to on-grid mode for different VES types

6. Conclusions

Research presented in this study led to the development of a non-stationary microgrid hybrid model. An associated microgrid operation optimisation method based on receding horizon control featuring a new method of DM is also featured. The incorporated VES allows for various gains. Compared to the system without the VES, bidirectional management ensures a 16% operational cost reduction and an average degree of energy shortage. Moreover, said cost stays the lowest regardless of the initial state of charge of PES or the length of operation in a given mode. The average state of charge of the VES does not depend on the initial state of PES, and the extent of VES-based DM is greater in off-grid mode. Notably, a bidirectional VES

achieves the best cost performance in terms of auxiliary generation, and it is in this aspect that the most significant financial benefits are obtained. Besides, the influence of disturbances proved to be linear-like and not distribution-dependent. An increase in control quality and economic benefits with prediction accuracy follows while significant circumstantial performance drops do not occur. The sensitivity of the solution showed that the chosen approach should allow for fine-tuning of the weighting matrices without a significant loss of performance. The proposed VES can accommodate a broader spectrum of non-critical demand and user needs. Also included is a mechanism ensuring equitable energy distribution and not burdening the user with the need to be mindful of VES. Depending on local conditions, only its specific types may be realizable. The conducted analysis has shown how it influences operating costs. This translates into wider opportunities for EMS systems, allowing for the integration of more renewable sources and fuller utilisation of renewable energy, which aligns with United Nations Sustainable Development Goal 7. The results are limited to the selected demand and generation scenarios set. Considering more scenarios prepared based on data sourced from multiple locations could lead to more pronounced results. Furthermore, an analysis of the sensitivity to changes in individual parameters could be beneficial for both microgrids with substantially different configurations and system longevity. Apart from this, all inaccuracy sources, including imperfect predictions, are represented by one random disturbance with a set distribution. This can negatively affect the obtained results in relation to actual working conditions. The model also does not consider the variability of the fuel price the generator uses, and the neighbourhood energy market is not considered. Control of the same operator over neighbouring microgrids is assumed, which limits applicability. In addition, extending the horizon would likely improve certain results but would involve simplifying the method for computational efficiency. The proposed solution is intended as an energy management system for microgrids operating under changing connection conditions and neighbouring with other microgrids. Especially in an environment where the pool of non-critical customers includes those who require considerable time to react, and a fair allocation of energy is essential. The authors intend to include more functionalities through further research and address discovered shortcomings. Future works suggest optimisation problem reformulation to allow for long-term prediction without disqualifying an increase in computational complexity and to include transmission loss mitigation.

CRediT authorship contribution statement

Grzegorz Maślak: Conceptualization, Formal analysis, Investigation, Methodology, Software, Visualization, Writing1—Original Draft, Writing1—Review and Editing. **Przemysław Orłowski:** Conceptualization, Formal analysis, Methodology, Resources, Supervision, Validation.

References

[1] M. J. B. Kabeyi and O. A. Olanrewaju, "Sustainable Energy Transition for Renewable and Low Carbon Grid Electricity Generation and Supply," *Frontiers in Energy Research*, vol. 9, 2022.

[2] C. Bordons, F. Garcia-Torres, and M. A. Ridao, *Model Predictive Control of Microgrids.* Springer Nature, Sept. 2019.

[3] M. Warneryd, M. Håkansson, and K. Karltorp, "Unpacking the complexity of community microgrids: A review of institutions' roles for development of microgrids," *Renewable and Sustainable Energy Reviews*, vol. 121, p. 109690, 2020.

[4] L. Ahmethodzic and M. Music, "Comprehensive review of trends in microgrid control," *Renewable Energy Focus*, vol. 38, pp. 84–96, Sept. 2021.

[5] A. Hirsch, Y. Parag, and J. Guerrero, "Microgrids: A review of technologies, key drivers, and outstanding issues," *Renewable and Sustainable Energy Reviews*, vol. 90, pp. 402–411, July 2018.

[6] M. H. Saeed, W. Fangzong, B. A. Kalwar, and S. Iqbal, "A Review on Microgrids' Challenges & Perspectives," *IEEE Access*, vol. 9, pp. 166502–166517, 2021. Conference Name: IEEE Access.

[7] M. Warneryd, M. Håkansson, and K. Karltorp, "Unpacking the complexity of community microgrids: A review of institutions' roles for development of microgrids," *Renewable and Sustainable Energy Reviews*, vol. 121, p. 109690, Apr. 2020.

[8] B. Zhou, B. Liu, D. Yang, J. Cao, and T. Littler, "Multi-objective optimal operation of coastal hydro-electrical energy system with seawater reverse osmosis desalination based on constrained NSGA-III," *Energy Conversion and Management*, vol. 207, p. 112533, Mar. 2020.

[9] B. Liu, B. Zhou, D. Yang, G. Li, J. Cao, S. Bu, and T. Littler, "Optimal planning of hybrid renewable energy system considering virtual energy storage of desalination plant based on mixed-integer NSGA-III," *Desalination*, vol. 521, p. 115382, Jan. 2022.

[10] Y. Mu, T. Yao, H. Jia, X. Yu, B. Zhao, X. Zhang, C. Ni, and L. Du, "Optimal scheduling method for belt conveyor system in coal mine considering silo virtual energy storage," *Applied Energy*, vol. 275, p. 115368, Oct. 2020.

[11] H. T. Nguyen, A. S. Al-Sumaiti, K. Turitsyn, Q. Li, and M. S. El Moursi, "Further Optimized Scheduling of Micro Grids via Dispatching Virtual Electricity Storage Offered by Deferrable Power-Driven Demands," *IEEE Transactions on Power Systems*, vol. 35, pp. 3494–3505, Sept. 2020.

[12] Q. Dang, D. Wu, and B. Boulet, "EV Fleet as Virtual Battery Resource for Community Microgrid Energy Storage Planning," *IEEE Canadian Journal of Electrical and Computer Engineering*, vol. 44, no. 4, pp. 431–442, 2021. Conference Name: IEEE Canadian Journal of Electrical and Computer Engineering.

[13] C. Wang, S. Fu, L. Zhang, Y. Jiang, and Y. Shu, "Optimal control of source–load–storage energy in DC microgrid based on the virtual energy storage system," *Energy Reports*, vol. 9, pp. 621–630, Dec. 2023.

[14] C. Xie, D. Wang, C. S. Lai, R. Wu, X. Wu, and L. L. Lai, "Optimal sizing of battery energy storage system in smart microgrid considering virtual energy storage system and high photovoltaic penetration," *Journal of Cleaner Production*, vol. 281, p. 125308, Jan. 2021.

[15] J. Joe, J. Dong, J. Munk, T. Kuruganti, and B. Cui, "Virtual storage capability of residential buildings for sustainable smart city via model-based predictive control," *Sustainable Cities and Society*, vol. 64, p. 102491, Jan. 2021.

[16] S.-J. Hahm, Y.-E. Jang, and Y.-J. Kim, "Virtual Battery Modeling of Air Conditioning Loads in the Presence of Unknown Heat Disturbances," *Energies*, vol. 15, no. 24, 2022.

[17] S. Wang, L. Lu, X. Han, M. Ouyang, and X. Feng, "Virtual-battery based droop control and energy storage system size optimization of a DC microgrid for electric vehicle fast charging station," *Applied Energy*, vol. 259, p. 114146, Feb. 2020.

[18] W. Xing, H. Wang, L. Lu, S. Wang, and M. Ouyang, "An adaptive droop control for distributed battery energy storage systems in microgrids with DAB converters," *International Journal of Electrical Power & Energy Systems*, vol. 130, p. 106944, Sept. 2021.

[19] A. Niromandfam, A. Movahedi Pour, and E. Zarezadeh, "Virtual energy storage modeling based on electricity customers' behavior to maximize wind profit," *Journal of Energy Storage*, vol. 32, p. 101811, Dec. 2020.

[20] A. R. Jordehi, "Optimisation of demand response in electric power systems, a review," *Renewable and Sustainable Energy Reviews*, vol. 103, pp. 308–319, Apr. 2019.

[21] H. Golmohamadi, "Demand-side management in industrial sector: A review of heavy industries," *Renewable and Sustainable Energy Reviews*, vol. 156, p. 111963, 2022.

[22] F. Garcia-Torres, A. Zafra-Cabeza, C. Silva, S. Grieu, T. Darure, and A. Estanqueiro, "Model Predictive Control for Microgrid Functionalities: Review and Future Challenges," *Energies*, vol. 14, p. 1296, Jan. 2021.

[23] H. Liu, A. Fan, Y. Li, R. Bucknall, and L. Chen, "Hierarchical distributed mpc method for hybrid energy management: A case study of ship with variable operating conditions," *Renewable and Sustainable Energy Reviews*, vol. 189, p. 113894, 2024.

[24] Y. Wang, W. Dong, and Q. Yang, "Multi-stage optimal energy management of multi-energy microgrid in deregulated electricity markets," *Applied Energy*, vol. 310, p. 118528, Mar. 2022.

[25] F. Jiao, C. Ji, Y. Zou, and X. Zhang, "Tri-stage optimal dispatch for a microgrid in the presence of uncertainties introduced by EVs and PV," *Applied Energy*, vol. 304, p. 117881, Dec. 2021.

[26] M. Shi, H. Wang, C. Lyu, P. Xie, Z. Xu, and Y. Jia, "A hybrid model of energy scheduling for integrated multi-energy microgrid with hydrogen and heat storage system," *Energy Reports*, vol. 7, pp. 357–368, Nov. 2021.

[27] R. Seshu Kumar, L. Phani Raghav, D. Koteswara Raju, and A. R. Singh, "Impact of multiple demand side management programs on the optimal operation of grid-connected microgrids," *Applied Energy*, vol. 301, p. 117466, Nov. 2021.

[28] W. C. Clarke, M. J. Brear, and C. Manzie, "Control of an isolated microgrid using hierarchical economic model predictive control," *Applied Energy*, vol. 280, p. 115960, Dec. 2020.

[29] M. A. Alarcón, R. G. Alarcón, A. H. González, and A. Ferramosca, "Economic model predictive control for energy management of a microgrid connected to the main electrical grid," *Journal of Process Control*, vol. 117, pp. 40–51, Sept. 2022.

[30] S. Noor, W. Yang, M. Guo, K. H. van Dam, and X. Wang, "Energy Demand Side Management within micro-grid networks enhanced by blockchain," *Applied Energy*, vol. 228, pp. 1385–1398, Oct. 2018.

[31] A. Nawaz, M. Zhou, J. Wu, and C. Long, "A comprehensive review on energy management, demand response, and coordination schemes utilization in multi-microgrids network," *Applied Energy*, vol. 323, p. 119596, Oct. 2022.

[32] D. P. e Silva, J. L. Félix Salles, J. F. Fardin, and M. M. Rocha Pereira, "Management of an island and grid-connected microgrid using hybrid economic model predictive control with weather data," *Applied Energy*, vol. 278, p. 115581, Nov. 2020.

[33] J. A. Basantes, D. E. Paredes, J. R. Llanos, D. E. Ortiz, and C. D. Burgos, "Energy Management System (EMS) Based on Model Predictive Control (MPC) for an Isolated DC Microgrid," *Energies*, vol. 16, p. 2912, Jan. 2023. Number: 6 Publisher: Multidisciplinary Digital Publishing Institute.

[34] G. Maślak and P. Orłowski, "Microgrid Operation Optimization Using Hybrid System Modeling and Switched Model Predictive Control," *Energies*, vol. 15, p. 833, Jan. 2022.

[35] C. K. Nayak, K. Kasturi, and M. R. Nayak, "Economical management of microgrid for optimal participation in electricity market," *Journal of Energy Storage*, vol. 21, pp. 657–664, Feb. 2019.

[36] S. Negri, F. Giani, A. Massi Pavan, A. Mellit, and E. Tironi, "MPC-based control for a stand-alone LVDC microgrid for rural electrification," *Sustainable Energy, Grids and Networks*, vol. 32, p. 100777, Dec. 2022.

[37] N. Houben, A. Cosic, M. Stadler, M. Mansoor, M. Zellinger, H. Auer, A. Ajanovic, and R. Haas, "Optimal dispatch of a multi-energy system microgrid under uncertainty: A renewable energy community in Austria," *Applied Energy*, vol. 337, p. 120913, May 2023.

[38] J. R. Nelson and N. G. Johnson, "Model predictive control of microgrids for real-time ancillary service market participation," *Applied Energy*, vol. 269, p. 114963, July 2020.

[39] B. V. Solanki, A. Raghurajan, K. Bhattacharya, and C. A. Cañizares, "Including Smart Loads for Optimal Demand Response in Integrated Energy Management Systems for Isolated Microgrids," *IEEE Transactions on Smart Grid*, vol. 8, pp. 1739–1748, July 2017. Conference Name: IEEE Transactions on Smart Grid.

[40] X. Yang, Y. Zhang, H. He, S. Ren, and G. Weng, "Real-Time Demand Side Management for a Microgrid Considering Uncertainties," *IEEE Transactions on Smart Grid*, vol. 10, pp. 3401–3414, May 2019. Conference Name: IEEE Transactions on Smart Grid.

[41] A. Nawaz, J. Wu, J. Ye, Y. Dong, and C. Long, "Distributed MPC-based energy scheduling for islanded multi-microgrid considering battery degradation and cyclic life deterioration," *Applied Energy*, vol. 329, p. 120168, Jan. 2023.

[42] J. Hu, Y. Shan, J. Guerrero, A. Ioinovici, K. Chan, and J. Rodriguez, "Model predictive control of microgrids – An overview," *Renewable and Sustainable Energy Reviews*, vol. 136, pp. 1–12, Oct. 2020.

[43] M. Farrokhifar, H. Bahmani, B. Faridpak, A. Safari, D. Pozo, and M. Aiello, "Model predictive control for demand side management in buildings: A survey," *Sustainable Cities and Society*, vol. 75, p. 103381, Dec. 2021.

[44] E.-E. Project, "Transparency platform data." https://transparency.entsoe.eu, 2022. Accessed: 2022-8-10.

[45] A. Rinaldi, S. Yilmaz, M. K. Patel, and D. Parra, "What adds more flexibility? An energy system analysis of storage, demand-side response, heating electrification, and distribution reinforcement," *Renewable and Sustainable Energy Reviews*, vol. 167, p. 112696, Oct. 2022.

[46] E. X, "Enel x demand side response." https://www.enelx.com/pl/en/demand-side-response, 2022. Accessed: 2022-10-21.

[47] F. Borrelli, A. Bemporad, and M. Morari, *Predictive Control for Linear and Hybrid Systems*. Cambridge, United Kingdom ; New York, NY, USA: Cambridge University Press, Feb. 2019.

[48] J. Löfberg, "Yalmip : A toolbox for modeling and optimization in matlab," in *In Proceedings of the IEEE International Symposium on Computer-Aided Control System Design*, (Taipei, Taiwan), 2004.

[49] G. O. LLC, "Gurobi optimizer reference manual." https://www.gurobi.com, 2022. Accessed: 2022-10-21.

[50] B. Zakeri and S. Syri, "Electrical energy storage systems: A comparative life cycle cost analysis," *Renewable and Sustainable Energy Reviews*, vol. 42, pp. 569–596, Feb. 2015.

[51] M. Yekini Suberu, M. Wazir Mustafa, and N. Bashir, "Energy storage systems for renewable energy power sector integration and mitigation of intermittency," *Renewable and Sustainable Energy Reviews*, vol. 35, pp. 499–514, July 2014.